PERGAMON

Geodynamics 27 (1999) 409–432

JOURNAL OF
GEODYNAMICS

Cenozoic volcanism and tectonics in the southern Tyrrhenian sea: space-time distribution and geodynamic significance

A. Argnani*, C. Savelli

Istituto per la Geologia Marina-CNR, Via Gobetti 101, 40129 Bologna, Italy

Accepted 27 June 1998

Abstract

Short-lived magmatic episodes separated in space and time are recognizable in the southern portion of the Tyrrhenian sea and on the island of Sardinia. Distinct episodes of subduction-related calcalkaline arc volcanism can be identified: on the island of Sardinia during the Oligo–Miocene (32–13 Ma), in the central part of the Tyrrhenian basin during the Pliocene (5–2 Ma), and in the active Aeolian arc, the southeastern basin margin, from the middle Pleistocene to Holocene (1–0 Ma).

The composition of the orogenic magmatic products in these arcs indicates the existence of a geochemical polarity of interarc type above a NW-dipping subducted slab.

NW–SE migration of calcalkaline volcanic activity was accompanied by the opening of the interarc Vavilov and Marsili sub-basins in late Tortonian to early Pliocene and in the upper Pliocene, respectively. During these time intervals, volcanic activity was mainly confined within the sub-basins with emplacement of MORB-like basalts.

Rift-related intra-plate volcanism occurred in the Pliocene (5–2 Ma), following the opening of the Vavilov basin, and resumed in the Quaternary (1.2–0.1 Ma) following the opening of the Marsili basin. This volcanism has a large areal distribution covering the island of Sardinia, the western Tyrrhenian margin, the Vavilov basin, the supposed central Tyrrhenian arc and, sporadically, the Marsili volcanic seamount.

The identified magmatic cycles allow constraints to be placed on the geodynamic evolution of the Tyrrhenian backarc basin which appears to be controlled by a rolling back subducted slab that becomes progressively steeper in time.

1. Introduction

The main geological features of the Mariana-type convergent margins (Uyeda, 1982) are extension and magmatism in the upper plate, up to the point where oceanic lithosphere is produced in

* Corresponding author. Fax: 0039-51-639-8940; e-mail: andrea@boigm2.bo.cnr.it

0264–3707/99/$ - see front matter
PII: SS0264-3707(98)00025-8

a backarc basin (BAB) setting, and a generally steep dip of the subducted slab. The thermo-chemical perturbation induced by the subducted lithosphere strongly affects the overlying mantle wedge and the upper plate. This process is accompanied by magmatism, tectonism, seismic activity and hydrothermal circulation of notable intensity which have attracted the attention of many specialist groups in the geological community (Jakes and White, 1972; Barberi et al., 1974; Dickinson, 1975; Isacks and Barazangi, 1977; Scott and Kroenke, 1980; Pearce, 1982; Tarney et al., 1982; Uyeda, 1982; Kobayashi, 1984; Channell and Mareschal, 1988; Yilmaz, 1990; Szabo et al., 1992; Innocenti et al., 1983; Hole et al., 1995; Clift et al., 1995).

Heterogeneity of magmatism and tectonic complexity characterize this kind of margin. Supra-subduction volcanism does not take place as a continuum but develops with discrete events; studies on the age, areal distribution and magmatic characters of the eruptive products provide an invaluable insight into the processes of subduction and back-arc extension (Scott and Kroenke, 1980; Clift et al., 1995). Generally, abundant volcanites of intraplate (IP) affinity are erupted in the late rifting stages, subsequent to the calcalkaline, subduction-related volcanic activity and to the back-arc basalt volcanism of MORB affinity (Tarney et al., 1982; Innocenti et al., 1983; Savelli, 1984; Yilmaz, 1990; Szabo et al., 1992; Hole et al., 1995; Pouclet et al., 1995).

The oceanic basement of the BABs is characterized by strong tectonic subsidence (Kobayashi, 1984) and its depth is greater than that of comparable age basement in 'normal' oceanic floors.

The Tyrrhenian Sea is a deep Neogene to Recent intra-orogenic basin that opened in the wake of the contemporaneously growing Apennine–Maghrebian fold-and-thrust belt. During its evolution it was affected by voluminous magmatic activity and by strong tectonic subsidence (Kastens et al., 1988; Savelli, 1988; Argnani, 1997). In order to explain the volcanic and tectonic processes related to the Tyrrhenian opening in internal position with respect to the Apennines and Sicilian Maghrebids, some authors proposed the marginal basin model derived from the western Pacific backarc basins (Barberi et al., 1974; Boccaletti and Manetti, 1978). In this frame, the evolution of the Tyrrhenian Sea and of the adjacent Apenninic orogenic wedge is described as being due to roll-back of the northwest-dipping Ionian lithosphere (Malinverno and Ryan, 1986; Doglioni, 1991). Other authors, however, favoured geodynamic models which do not contemplate subduction and are, instead, based on the diapiric uprise of hot asthenosphere (Locardi, 1982; Wezel, 1985; Locardi and Nicolich, 1992), on lithospheric scale extension over low-angle faults (Lavecchia, 1988; Wang et al., 1989; Crisci et al., 1991), or on lateral extrusion due to convergence between the European and the African plates (Mantovani et al., 1992).

The nature and distribution of magmatism (Savelli, 1988; Argnani et al., 1995), the character of deep and intermediate seismicity (Anderson and Jackson, 1987; Giardini and Velona', 1991; Selvaggi and Chiarabba, 1995), and the concomitant extension in the Tyrrhenian and contraction in the Apennines (Patacca et al., 1992) has led us to prefer subduction related models (Malinverno and Ryan, 1986; Channell and Mareschal, 1988).

The purpose of this paper is to illustrate the time-space distribution, the chemistry and the tectonic setting of the Cenozoic volcanism in the south Tyrrhenian basin and on the adjoining Island of Sardinia. The episodicity of tectonics and volcanism provides useful constraints for a better understanding of the subduction process and of backarc evolution in the Sardo–Tyrrhenian region (STR).

2. Geological setting

The triangular-shaped Tyrrhenian sea is divided into a shallower northern part and a deeper southern part. In the deeper southern Tyrrhenian basin, which is the object of this study (Fig. 1), mantle derived basic magmatism developed, whereas acidic crustal derived magmatism prevailed in the northern Tyrrhenian basin. The amount of extension in the southern basin, where areas of oceanic-like lithosphere are present, was presumably greater than that in the northern basin. Estimates of migration rates of the extension-related magmatism are about 4.8 cm/a in the southern deep basin, but only 1.3 cm/a in the northern shallow area (Civetta et al., 1978; Savelli, 1988; Patacca and Scandone, 1989; Serri, 1990).

The southern Tyrrhenian basin is characterized by deep water (3600–3000 m), high heat flow (Mongelli et al., 1992) and a marked positive Bouguer gravimetric anomaly, as well as high intensity (up to 1500 nT) and small amplitude magnetic patterns (Della Vedova et al., 1984; Faggioni et al., 1995). The Vavilov and Marsili sub-basins represent the deeper portions of the southern Tyrrenian sea and are characterized by relatively thin crust (Moho shallower than 10 km; Nicolich and Dal Piaz, 1991). Large volcanic seamounts, 20–45 km long and elongated roughly north-south, are emplaced on the deep water sea floor. The Vavilov and Marsili basins are separated one from the other by the north–south trending bathymetric high where the Glauco and the Issel seamounts are located. Across this high an inter-basinal deepening of the Moho from 8–10 to 15 km, roughly extending from the island of Ustica to Issel seamount, has been observed (Steinmetz et al., 1983). Within the sub-basins, sediments are 600 m, and locally up to 900 m, thick and ODP data indicate that sedimentation rates increased from late Pliocene to Pleistocene in concomitance with a large input of volcaniclastics.

The results of the Deep Sea Drilling Project (DSDP) Legs 42 and Ocean Drilling Program (ODP) 107, together with geophysical investigations, indicate that accretion of oceanic-type crust took place in the Vavilov and Marsili sub-basins. Such oceanic-like areas are bounded by the Aeolian volcanic arc to the east and by a well developed continental rise, adjacent to the island of Sardinia, to the west.

3. Timing of tectonic and magmatic events

3.1. Arc volcanism migration

Arc volcanism occurred in the Island of Sardinia, the Tyrrhenian western border, 32–13 Ma ago (Savelli et al., 1979) and migrated to the Islands and Seamounts of the Aeolian area where calcalkaline (CA) volcanics are 1–0 Ma old (Figs 1 and 2).

A supposed arc of Pliocene age (5–2 Ma) is located in the central part of the Tyrrhenian sea, between the sub-basins of Vavilov and Marsili (Kastens et al., 1988; Savelli, 1988; Ferrari and Manetti, 1993). When compared to those of the Aeolian and Sardinian arcs, the CA volcanic activity of the central arc appears to be less intensive, and defined volcanic edifices are located only at the extremities of the structure. The volcanic seamount Anchise, the rhyolites of the island of Ponza and, perhaps, also the sequence of basalts and andesites recovered from deep drillings in the Volturno river plain, north of the presently active Phlegrean Fields, belongs to the central arc

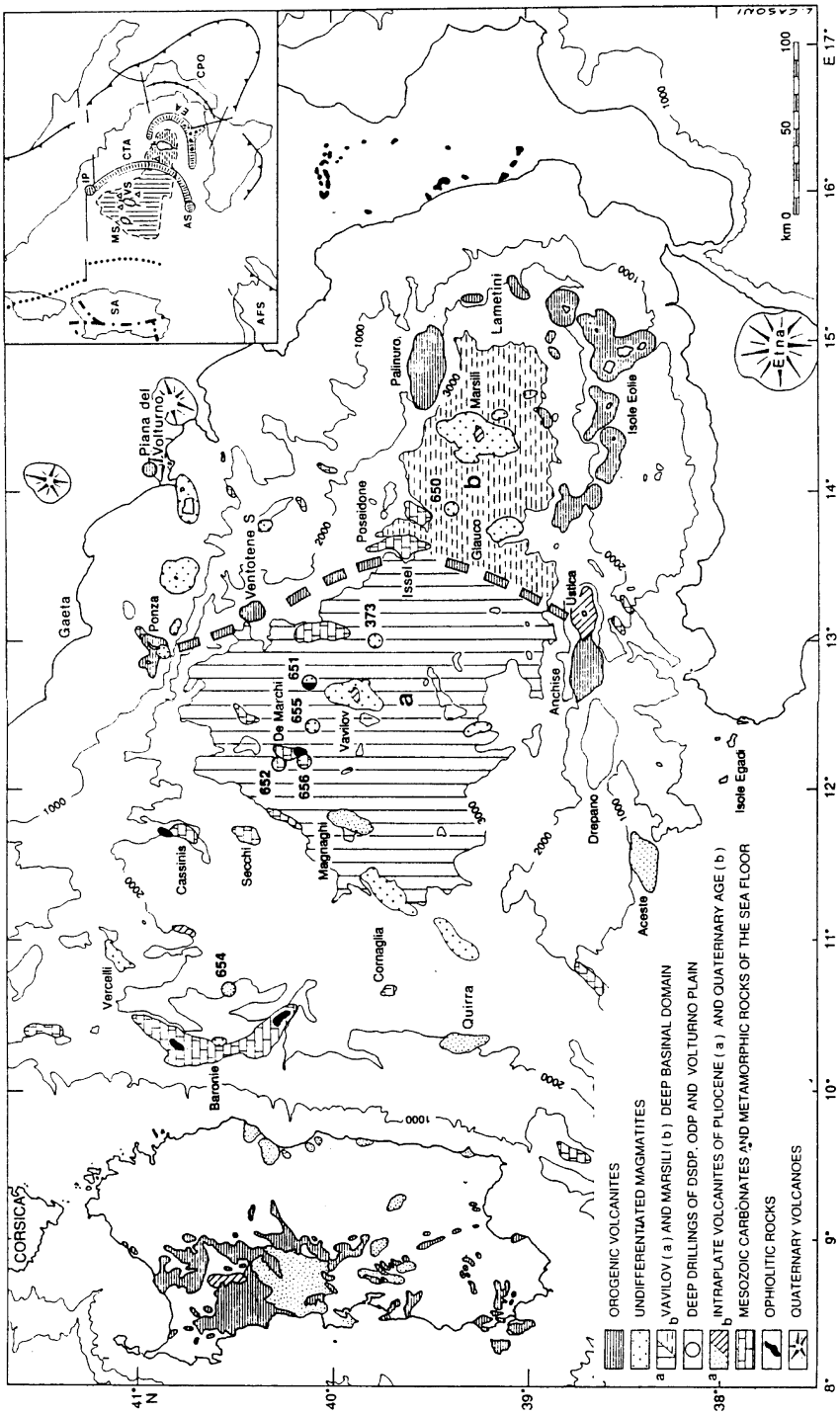

Fig. 1. Location of the study area showing the orogenic volcanic arcs, the Vavilov (a) and Marsili (b) sub-basins, and the distribution of magmatism in the Sardo–Tyrrhenian region.

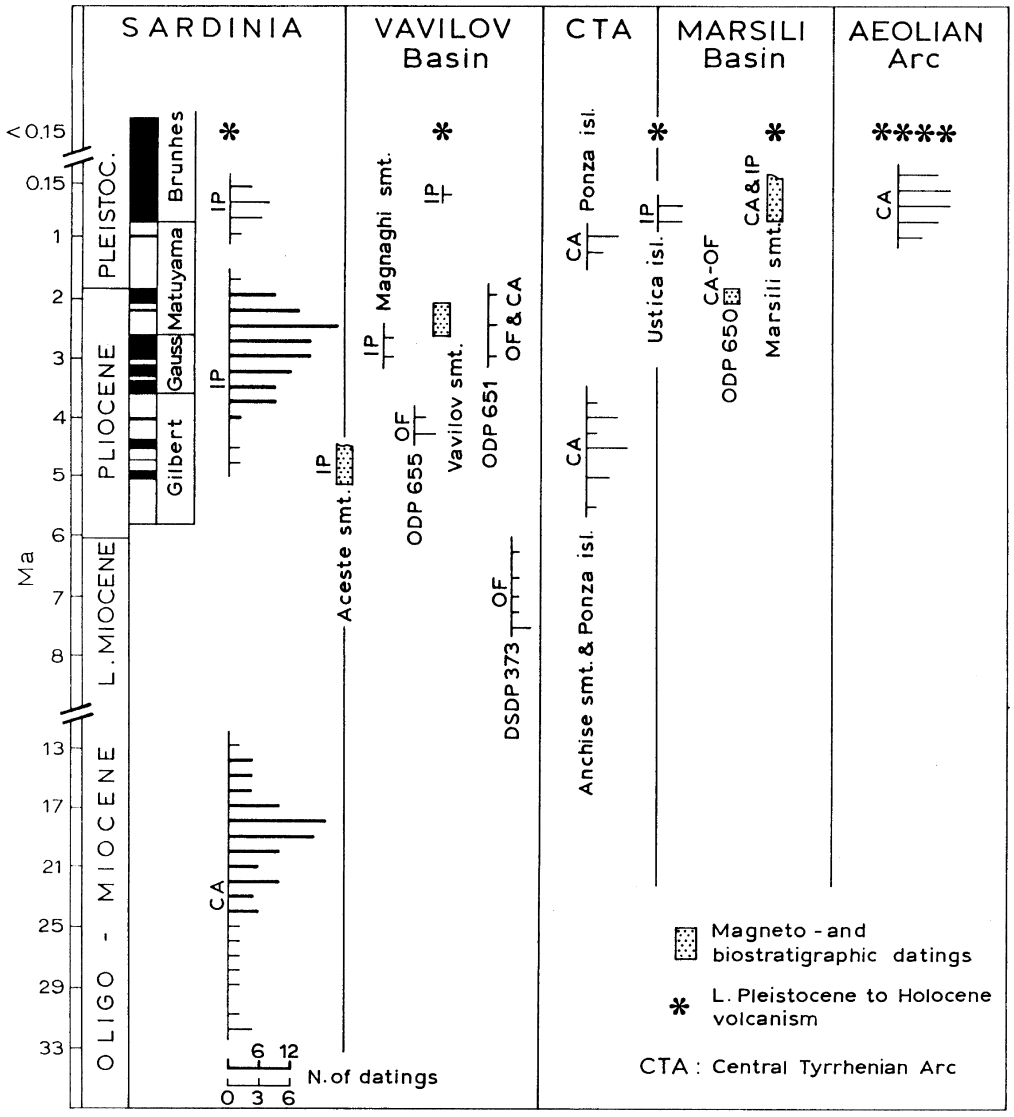

Fig. 2. Scheme of the stratigraphic and geochronological correlation of magmatic products in the Sardo–Tyrrhenian region. Horizontal bars represent number of radiometric datings. The large time gap between Oligo–Miocene and Mio–Pleistocene volcanism is related to the closure of the Algero–Provencial backarc basin and the opening of the Tyrrhenian basin.

volcanic sequence. The Glauco and Ventotene-south volcanic seamounts are located in the central portion of the arc; although the geochemistry and age of their products have not been ascertained, we assume that these edifices are part of the central magmatic arc. On the other hand, the Issel and Poseidon seamounts, consisting of metamorphic rocks, may represent the continental basement of this arc Fig. 1.

The composition of the magmatic products of the active Aeolian volcanic arc is more variable

than that of the old volcanites of the continental margins of Sardinia and of the central Tyrrhenian (Fig. 3; Table 1). The chemistry of the different CA episodes (Argnani et al., 1995) indicates that there is a distinctive increment of the potassic alkalinity from the Sardinian island to the Aeolian arc. Volcanites of shoshonitic affinity are abundant among the basic rocks (basalts and basaltic andesites) of the Aeolian area whereas they are absent among the basic rocks of the Oligo–Miocene magmatic episode of Sardinia.

Following predicted relationships of magma source depth with the K content of volcanic products (Dickinson, 1975), this interarc geochemical polarity suggests variation in the geometry of subducted lithosphere.

3.2. The backarc spreading

The migration of arc volcanism was accompanied by two episodes of emplacement of oceanic-like crust in two sub-basins (Fig. 4). The first episode occurred from late Miocene (8 Ma) to early Pliocene (4 Ma) in the Vavilov sub-basin and the second took place during late Pliocene (2–1.6 Ma) in the Marsili sub-basin. In each case, BAB opening occurred prior to the onset of the corresponding arc volcanism to the east. The chemical data of representative basalts of backarc setting are listed in Table 2 which shows that the deep-seated basalts from the DSDP Leg 373 consist of high- and low-Ti lavas.

The Ti–Zr discriminating plot of tectonic setting (Fig. 5) shows that igneous basement rocks of drill hole DSDP 373 and drill hole 655 of the ODP Leg 107 fall in the field for ocean-floor volcanites (Barberi et al., 1978; Dietrich et al., 1978; Beccaluva et al., 1990; Bertrand et al., 1990). The lavas of two basalt units recovered in the drill hole 651 also belong to this field. However, the upper unit lavas of hole 651 are chemically different from the lavas of the lower unit. Their K contents are high in comparison to those of basalts from a MOR setting (Fig. 6), and their Rb and Th values of 30–35 (Table 2) and 4–9.5 pm, respectively (Beccaluva et al., 1990), indicate a more CA affinity. Also the K, Rb and Th values of the basalts of the site 650 in the Marsili basin are high, and more akin to those of basic products of the CA series.

The potassium and related LILE contents of the basalts in sites DSDP 373 and ODP 655 are lower than those of sites ODP 650 and 651. The enrichment in LILE (K, Rb and Th) of the rocks of sites 650 and 651 is likely to be a consequence of the enhanced chemical modifications induced by fluids derived from the subducted material on E-MORB-like parental magma.

3.3. The intra-plate volcanism

Intra-plate (IP) rift-related volcanism occurred in two episodes and is distributed over a large area, extending from Sardinia to the southeastern Tyrrhenian Sea (Figures 1–2). In Sardinia this volcanism was initiated 5 Ma ago, post-dating both the Oligo–Miocene CA episode and the OF volcanism of the Vavilov basin, and continued until 2 Ma ago. This Pliocene activity is therefore coeval with the CA volcanism of the supposed intermediate arc. Volcanic activity stopped during the emplacement of oceanic lithosphere in the Marsili basin and then resumed again in concomitance with the Aeolian arc CA volcanism (1–0 Ma).

The chemical data of representative lavas of IP tectonic setting are listed in Table 2.

The volcanites of different magmatic and geodynamic significance, which affected the island of

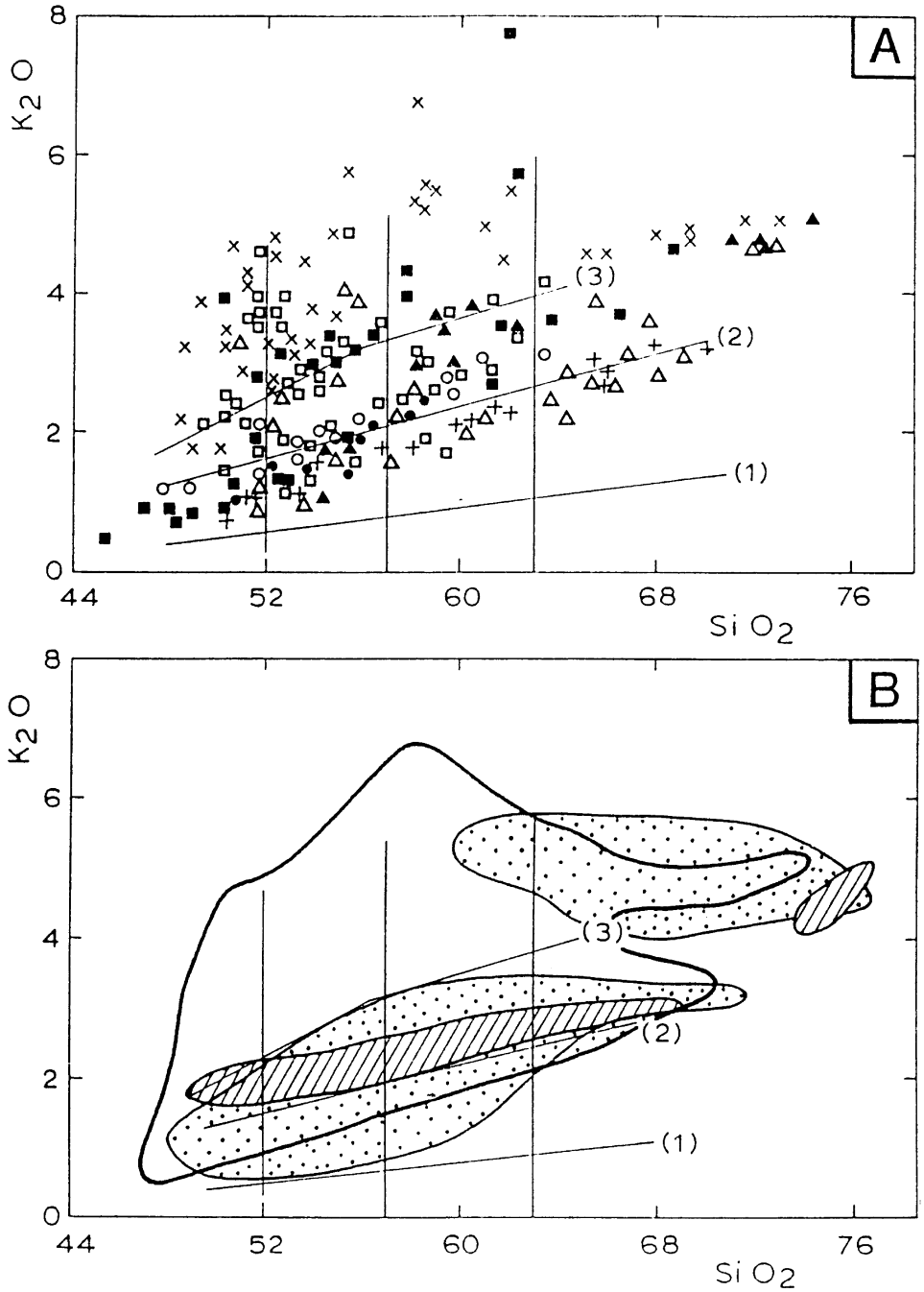

Fig. 3. K_2O–SiO_2 variation diagram of orogenic rocks of the Aeolian volcanic arc (**A**), and of the Central Tyrrhenian and Sardinia arc (**B**) on the basis of 363 rock analyses (Argnani et al., 1995). Boundary lines of the main volcanic associations: (1) = boundary between low-K (tholeiitic) and medium-K (calcalkaline s.s.) series, (2) = boundary between medium-K and high-K series (Le Maitre, 1989), (3) = boundary between high-K and shoshonitic series (Peccerillo and Taylor, 1976). Legend (**A**): (■) = Aeolian volcanic seamounts; (□) = island of Stromboli; (**x**) = island of Vulcano; (+) = island of Salina; (△) = island of Panarea; (▲) = island of Lipari; (○) = island of Filicudi; (●) = island of Alicudi; (**B**): thick line = field of the Aeolian volcanites; dots = fields of the Sardinian volcanites; stripes = fields of the volcanites of the central Tyrrhenian arc.

Table 1
Representative chemical analyses of the calcalkaline episodes of arc volcanism in the Sardo–Tyrrhenian region; major and trace elements in wt % and in ppm, respectively (refer. in Argnani et al., 1995)

Sardinia										Central Tyrrhenian arc			
Sample	a501	a714	a503	al1	ach53	a567	al3	nu371	co362	an122	napa3	fb1–5	po46B
ser. aff.	ca	ca	hk	sho	ca	hk	sho	sho	com	hk	hk	hk	hk
SiO2	50.58	52.71	53.03	58.41	58.86	59.23	62.09	70.17	71.67	51.78	54.13	74.78	75.10
TiO2	1.03	0.74	0.96	0.78	0.61	0.65	0.79	0.43	0.40	1.24	0.80	0.34	0.19
Al2O3	17.90	13.57	20.42	18.37	18.61	17.16	18.25	14.47	12.23	17.66	18.20	13.27	13.68
Fe2O3	1.49	1.32	1.02	0.84	1.98	0.91	0.69	3.04	3.86	6.99	2.04	1.16	1.24
FeO	8.96	7.92	6.11	5.05	4.89	5.48	4.15	0.26	0.79	2.18	5.21	0.98	0.57
MnO	0.19	0.13	0.15	0.12	0.20	0.12	0.09	0.03	0.12	0.09	0.09	0.07	0.04
MgO	5.52	9.91	8.00	1.83	2.22	3.32	0.43	0.41	0.34	4.25	4.59	0.32	0.10
CaO	10.34	8.93	8.20	7.09	7.05	7.09	5.78	1.26	0.27	10.61	10.01	1.32	1.40
Na2O	2.07	1.57	3.01	3.09	2.95	2.86	3.05	4.05	4.83	3.20	2.36	3.00	2.99
K2O	0.80	1.03	1.79	3.73	1.84	2.10	4.26	5.14	4.84	1.72	2.26	4.34	4.66
P2O5	0.30	0.18	0.25	0.28	0.18	0.23	0.27	0.08	0.04	0.33	n.a	0.04	0.03
LOI	1.99	2.97	1.11	1.71	0.59	1.15	1.54	0.66	0.70	1.65	1.77	5.49	4.49
Rb	19	33	45	137	81	70	99	191	257	41	74	177	283
Sr	291	171	401	414	338	340	407	139	9	451	664	187	228
Y	20	17	27	23	16	33	18	42	100	31	23	24	42
Zr	58	53	101	171	109	143	161	442	1100	118	54	160	244
Nb	5	5	9	12	6	9	11	31	135	16	7	12	23
Ba	143	256	303	353	615	320	396	872	69	n.a	465	541	380
La	7	9	17	26	20	23	27	61	111	n.a	24	35	57
Ce	16	18	35	52	36	48	54	109	210	n.a	45	52	94
Ni	15	220	10	15	14	14	11	n.a.	n.a.	n.a	18	5	n.a
Cr	48	701	14	36	5	26	21	9	6	n.a	50	6	32
Aeolian arc													
Sample	fil11	st1	alc31	st2	lp1	st144	lp33	st59	vu44	st41	lp39	pan08	lp9
ser.aff.	ca	sho	ca	ca	ca	ca	sho	hk	le.teph	hk	sho	hk	hk
SiO2	49.47	49.77	50.55	52.66	53.33	53.93	55.63	56.74	58.60	60.02	60.25	65.34	71.00
TiO2	0.74	0.99	0.67	0.63	0.67	0.77	0.80	0.71	0.60	0.78	1.00	0.56	0.15
Al2O3	16.76	17.30	15.41	17.46	16.79	17.17	17.83	16.88	16.30	16.93	17.57	15.69	13.20
Fe2O3	3.30	3.65	2.63	4.34	1.18	3.21	1.07	2.70	3.75	2.10	0.81	5.56	n.a
FeO	6.40	5.20	5.40	4.84	7.05	4.00	6.42	4.15	2.45	3.47	4.84	n.a.	2.70
MnO	0.18	0.17	0.15	0.17	0.15	0.15	0.14	0.13	0.12	0.12	0.11	0.10	0.07
MgO	6.99	5.62	9.61	5.23	5.88	6.13	3.19	4.81	2.60	3.14	2.45	2.15	1.10
CaO	12.02	11.31	10.91	9.62	10.64	9.65	7.31	7.97	4.90	6.47	6.09	4.56	2.10
Na2O	1.97	2.73	2.28	2.15	2.09	2.59	2.63	3.15	4.10	3.39	2.79	3.23	3.80
K2O	0.96	2.15	1.33	0.96	1.33	1.33	3.04	1.78	5.60	2.83	3.47	2.68	4.80
P2O5	0.25	0.53	0.25	0.17	0.22	0.18	0.29	0.25	0.34	0.25	0.24	0.13	0.06
LOI	0.96	0.58	0.82	1.76	0.67	0.83	1.63	0.66	0.40	0.43	0.68	1.64	0.4
Rb	23	72	34	19	42	39	78	47	235	83	122	97	280
Sr	604	742	685	556	565	427	739	491	930	500	637	384	181
Y	21	30	16	18	19	22	22	22	25	27	21	29	n.a.
Zr	51	184	81	41	112	106	138	131	277	192	139	131	180

Table 1.—*continued*

Aeolian arc													
Sample	fil11	st1	alc31	st2	lp1	st144	lp33	st59	vu44	st41	lp39	pan08	lp9
ser.aff.	ca	sho	ca	ca	ca	ca	sho	hk	le.teph	hk	sho	hk	hk
Nb	4	22	7	2	4	6	11	15	n.a.	16	13	9	n.a.
Ba	250	1094	390	310	289	328	752	500	971	825	711	567	200
La	16	48	23	12	19	26	35	33	58	45	38	30	n.a.
Ce	36	97	42	23	41	49	69	57	143	85	74	48	n.a.
Ni	32	42	123	29	53	55	24	34	12	11	18	9	30
Cr	99	63	496	69	157	226	67	123	23	16	38	15	20

ser. aff.= serial affinity; ca=calcalkaline medium potassic; hk=calcalkaline high-potassic; sho=shoshonitic (comprising the peralkaline rhyiolites). Com=comendites; le.teph.= leucite tephrites.

Sardinia and its Tyrrhenian margin during the episodes of 32–13; 5–2 and 1–0 Ma, are plotted in the Na_2O+K_2O vs SiO_2 discrimination diagram (Fig. 7). Figure 7 shows that the Oligo–Miocene calcalkaline rocks of Sardinia fall in the subalkaline field, whereas most of the IP volcanites of the Pliocene episode of Sardinia are of a more alkaline nature with the rocks of the Monti Ferru volcanic complex characterised by marked potassic alkalinity (phonolites) (Table 2). However, a consistent portion of the eruptions of this episode have sub-alkaline composition (basaltic andesites). In fact, the Monte Arci volcanic complex is made up of basalts, andesites, dacites and rhyolites of subalkaline affinity as well as of a series of alkaline rocks, consisting of hawaiites, mugearites and alkaline trachytes (Cioni et al., 1982). The ODP site 654 basalts of the late Pliocene in the west Tyrrhenian margin have subalkaline affinity (Table 2).

The IP volcanites of the Quaternary episode of NW Sardinia (the Logudoro district; Macciotta and Savelli, 1984) and of the west Tyrrhenian margin (Keller, 1981) are entirely of alkaline nature. In general, on the island of Sardinia and on its eastern margin the IP volcanites become more alkaline with time. The Pliocene episode consists of subalkaline and alkaline rocks—in Sardinia the basaltic andesites are topped locally by alkalic rocks—and the less voluminous Pleistocene episode is made up of alkaline lavas only.

In the $TiO_2 \times 5$–Al_2O_3–MgO diagram (Fig. 8) for basic and intermediate rocks of Cabanis et al. (1990) the products of the two IP volcanic episodes of Sardinia and of its eastern margin are distinguished from those of the old CA episode.

The two IP volcanic episodes also took place in the large volcanic seamounts emplaced on the Tyrrhenian basin floor (Table 2, Figs 1 and 2). Not much is known about the chemistry of these edifices, however the bulk of Magnaghi volcano appears to be made up of IP basalts of Pliocene age (3.0–2.7 Ma), whereas rocks of this tectonic affinity, but of Quaternary age (0.4–$<$0.2 Ma), occur locally on the ridges of the seamounts of Vavilov and Marsili (Selli et al., 1977; Robin et al., 1987; Faggioni et al., 1995). The bulk of Vavilov is made up of pillow lavas with age belonging to the pre-Olduvay portion of the Matuyama polarity period (Fig. 2); however, their composition has not been ascertained.

Also the volcanic edifice of Ustica was constructed by IP volcanics (Table 2) belonging to the Quaternary episode (0.79 to $<$0.13 Ma —post Tyrrhenian; Calanchi et al., 1984; Cinque et al.,

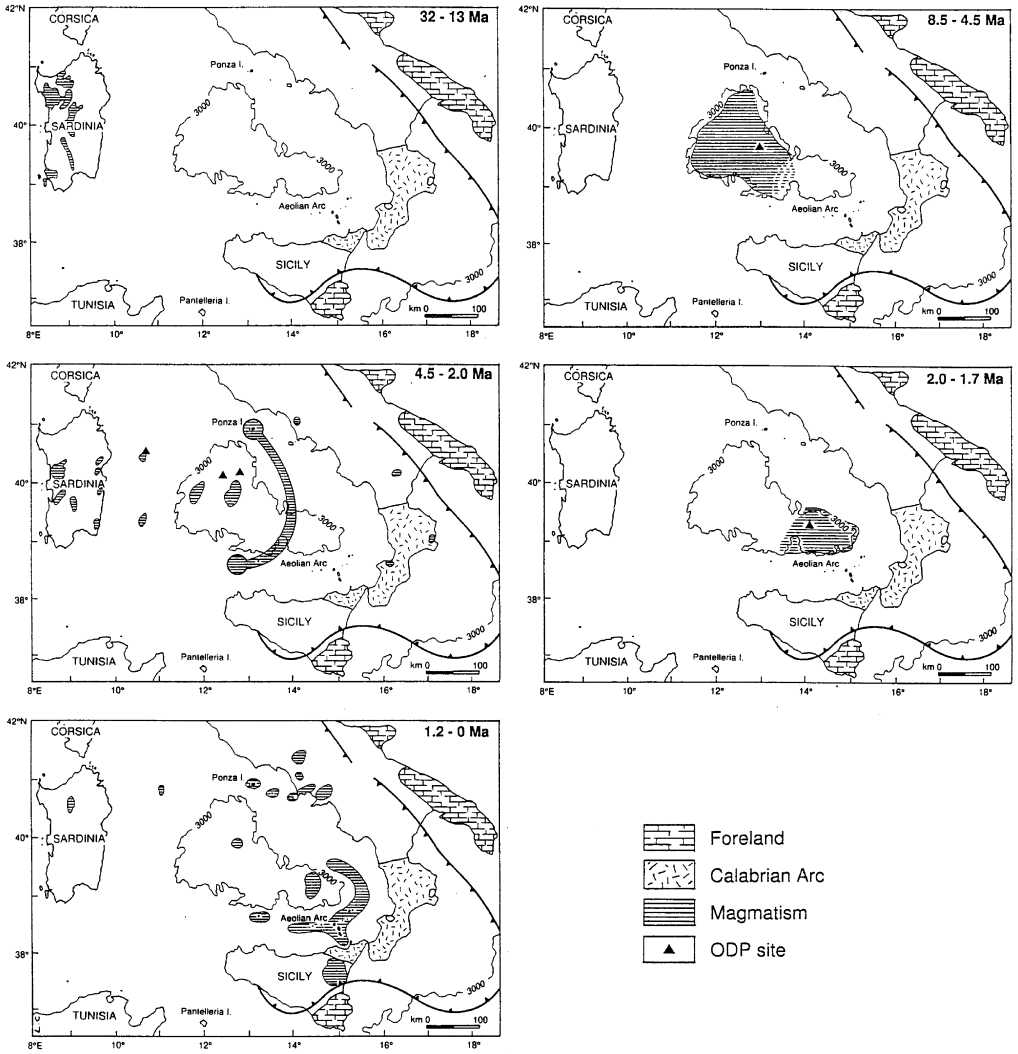

Fig. 4. Sketch maps showing the space-time distribution of Cenozoic volcanism in the Sardo–Tyrrhenian region during the time intervals 32–13 Ma (Oligo–Miocene), 8.5–4.5 (upper Miocene), 4.5–2.0 Ma (Pliocene), 2.0–1.7 (uppermost Pliocene) and 1.2–0 Ma (middle Pleistocene–Holocene). Both the two volcanic episodes of spreading in the deep basins of Vavilov and Marsili, respectively of the upper Miocene and the uppermost Pliocene, took place when the adjoining arcs where quiescent.

Table 2
Representative chemical analyses of volcanites from the Sardo–Tyrrhenian region (major and trace elements in wt % and ppm, respectively); their selection is from a file consisting of 269 rock analyses, of which 168 refer to Sardinian products of the IP activity of Pliocene and Pleistocene age. The orogenic rocks from the volcanic arcs of Sardinia, the Central Tyrrhenian and Eolie (Argnani et al., 1995) are not included

Vavilov basin									seamounts			Marsili basin			Marsili smt.			W Tyrrhenian margin		
Sample	373l.Ti	373h.Ti	655–1–4	655–4–1	655–12	651–44	651–49	651–53	Magn.	Vv.T72	Vav3x	650–67	\67b	650–69	M1–3	1657	CT69		654–1	654–2	RC–9–2
Affinity	OF b.	OF b.	OF b.	OF b.	OF b.	OF b.	CA b.	CA b.	IP b.	IP b.	IP b.	CA an.	CA an.	CA b.	CA b.	CA an.	IP b.		IP b.	IP b.	IP b.
Age\Ma	8\6	8\6	4.3	4.3	4.3	2.6	2.6	2.6	3–2,5	<0,8	<0,4	1,9–1,7	1,9–1,7	1,9–1,7	<0,8	<0,2	<0,2		2.0	2.0	<0,1
SiO2	47.80	51.00	51.31	49.05	51.30	53.06	53.99	53.70	49.38	48.05	48.87	58.00	57.54	54.61	47.15	59.95	46.63		54.12	54.45	48.82
TiO2	1.05	1.68	1.49	1.59	1.26	1.56	1.35	1.30	1.97	3.27	2.36	1.31	1.25	1.21	0.61	0.96	2.30		1.58	1.54	2.24
Al2O3	19.40	17.00	16.25	17.18	16.62	16.88	15.75	16.23	19.93	18.00	17.59	20.77	20.61	18.01	18.60	16.76	15.82		14.80	15.12	16.41
Fe2O3	8.65	10.20	9.88	10.83	9.26	8.84	8.73	7.92	2.36	3.08	3.54	6.07	7.34	9.28	7.49	6.23	2.05		3.42	9.61	1.72
FeO	n.a.	n.a.	n.a.	n.a.	n.a.	n.a.	n.a.	n.a.	7.85	8.96	6.42	n.a.	n.a.	n.a.	n.a.	n.a.	9.22		6.19	n.a.	9.30
MnO	0.16	0.17	0.13	0.00	0.13	0.09	0.12	0.13	0.16	0.17	0.17	0.06	0.04	0.08	0.12	0.12	0.17		0.13	0.12	0.16
MgO	8.60	6.75	7.25	6.62	7.46	8.70	7.27	7.50	3.34	4.14	7.91	2.44	2.00	4.06	7.04	2.00	8.82		6.74	7.09	5.70
CaO	11.80	8.74	9.55	10.57	10.00	5.49	7.22	7.26	10.76	10.20	7.67	6.48	5.56	6.79	13.98	4.44	12.09		7.15	7.10	7.28
Na2O	2.92	4.29	3.59	3.55	3.46	3.84	3.64	3.46	3.34	3.15	3.86	4.10	4.63	4.47	2.12	4.82	2.27		3.50	3.52	4.45
K2O	0.29	0.34	0.35	0.27	0.34	0.84	1.72	2.23	0.50	0.58	1.26	0.67	0.88	1.24	0.56	3.02	0.37		0.59	0.60	1.60
P2O5	0.14	0.24	0.20	0.14	0.17	0.15	0.20	0.27	0.41	0.42	n.a.	0.07	0.13	0.24	0.25	0.44	0.25		0.18	0.19	0.49
LOI	4.34	2.70	1.86	1.46	1.70	3.19	2.29	2.13	1.34	1.03	1.55	5.48	3.50	3.16	1.84	0.90	1.81		1.60	0.66	1.80
Rb	3.3	3.5	2.5	2.5	3	5	30	35.5	10	10.5	13	10	9	19.5	13	87	9		7	7	26
Sr	230	201	195	188	200	272	237	358	295	338	415	323	337	392	597	392	311		478	471	506
Y	24	37	26	30	24	29	26	24	39	42	34	11	14	20	16	36	24		15	15	20
Zr	70	130	107	97	99	131	118	133	228	228	162	105	78	92	53	194	139		75	80	156
Nb	3.1	6.5	6.0	6.0	6.0	10.0	7.0	10.0	16.0	21.0	35.0	5.0	4.0	4.0	6.0	22.0	18.0		8	11	n.a.
Ba	64	63	62	71	61	151	172	255	n.a.	99	402	120	160	216	207	1167	n.a.		152	155	480
La	5.2	8.1	5.4	4.9	5	13.5	11.6	17.2	n.a.	17	18.5	9.3	8.3	13.7	14	43	n.a.		9	8	n.a.
Ce	11.8	18.5	14.2	12.8	13.5	29.5	25.5	36.6	n.a.	42.8	38.6	21	19	29	30	78	n.a.		20	20	n.a.
Ni	83	52	107	66	123	50	52	71	30	32	122	206	164	97	77	5	184		181	172	82
Cr	222	141	141	118	188	97	81	218	79	35	127	400	389	229	129	13	357		273	248	80
Refer.	\1	\1	\2	\2	\2	\2	\2	\2	\3	\3	\4	\5	\5	\5	\6	\6	\3		\5	\5	\7

Sardinia															Aceste smt.				Ustica Island		
Sample	av.−68s.	av.18s.	130	168	179	158	77	V28A	423	42	239DB	412	LL85	A404	Ha 3	Mu 4	Tr 2	Rh	SH1	108	167
Affinity	IP ak b.	IP s.b.	IP sb.	IP an.	IP da.	IP rh.	IP ak b.	IP ak b.	IP ak b.	te–ph.	ph–te.	ph.	IP ak b.	IP ak b.	IP ha.	IP mu.	tr.	rh. IP	ak. b. IP	ak. b.	IP tr.
Age	5–1.9	5–1.9	5–1.9	5–1.9	5–1.9	5–1.9	5–1.9	5–1.9	5–1.9	5–1.9	5–1.9	5–1.9	<0.12	0.6	5–1.9	5–1.9	5–1.9	5–1.9	<1	<1	<1
SiO2	50.9	54.36	53.21	60.49	65.42	71.93	51.30	50.57	48.03	55.81	56.97	59.47	49.08	51.34	54.34	56.52	63.96	66.30	49.78	50.50	61.65
TiO2	2.16	1.59	1.57	1.16	0.97	0.42	1.74	2.28	2.52	1.47	1.12	0.27	2.10	2.54	1.46	1.87	0.35	0.22	1.51	1.51	0.55
Al2O3	16.04	15.65	16.70	15.27	14.57	14.42	17.33	16.00	16.29	20.55	22.32	20.12	15.39	16.28	18.81	19.08	17.72	13.96	17.66	19.03	19.47
Fe2O3	n.a.	n.a.	1.15	1.28	1.30	0.53	2.81	6.33	3.51	4.52	2.94	1.52	n.a.	0.00	6.62	4.68	2.95	3.24	4.53	4.98	2.31
FeO	9.04	8.52	7.53	5.00	3.31	1.59	5.11	2.94	6.57	1.10	1.41	0.64	9.17	9.17	n.a.	n.a.	n.a.	n.a.	5.06	3.55	2.28
MnO	n.a.	n.a.	0.13	0.11	0.10	0.09	0.12	0.13	0.14	0.10	0.11	0.12	0.14	0.13	0.09	0.06	0.02	0.05	0.15	0.15	0.18
MgO	6.38	5.91	6.78	4.36	3.04	0.48	6.47	5.98	7.63	1.69	1.00	0.24	6.84	4.64	2.28	1.96	0.03	0.07	5.53	4.85	0.80
CaO	7.17	6.88	7.05	4.66	3.23	1.17	6.49	6.85	8.17	4.42	3.51	1.14	7.96	6.68	9.14	7.58	0.36	1.00	9.02	9.68	2.35
Na2O	4.09	3.84	3.73	3.82	3.69	3.43	4.17	4.12	2.78	6.44	4.53	8.77	3.62	4.10	3.98	4.42	6.94	2.66	3.89	3.72	6.89
K2O	2.47	1.20	0.87	1.93	3.57	5.34	2.64	2.18	2.24	3.26	5.93	6.40	2.60	2.76	1.33	2.36	5.32	4.26	1.10	1.21	3.29
P2O5	0.59	0.23	0.28	0.14	0.18	0.12	0.65	0.61	0.61	0.41	0.31	0.04	0.67	0.66	0.18	0.35	0.06	0.04	0.47	0.52	0.23
LOI	n.a.	n.a.	1.00	1.77	0.62	0.48	1.18	1.51	1.32	3.58	2.07	0.67	0.96	0.60	1.73	1.12	2.29	6.20	1.30	n.a.	n.a.
Rb	47	29	21	71	177	206	63	n.a.	n.a.	n.a.	n.a.	n.a.	61	56	21	66	282	260	20	30	61
Sr	946	512	463	386	435	153	738	n.a.	n.a.	n.a.	n.a.	n.a.	858	1126	308	321	39	46	740	789	333
Y	22	23	n.a.	n.a.	n.a.	n.a.	n.a.	n.a.	n.a.	n.a.	n.a.	n.a.	21	n.a.	32	35	93	48	27	25	26
Zr	170	121	126	122	146	258	253	n.a.	n.a.	n.a.	n.a.	n.a.	212	n.a.	193	199	301	223	144	138	320
Nb	52	20	n.a.	n.a.	n.a.	n.a.	n.a.	n.a.	n.a.	n.a.	n.a.	n.a.	51	n.a.	21	24	89	30	42	24	n.a.
Ba	n.a.	n.a.	334	357	463	1020	938	n.a.	n.a.	n.a.	n.a.	n.a.	1030	1101	n.a.	n.a.	n.a.	n.a.	n.a.	n.a.	n.a.
La	n.a.	n.a.	20	26	36	73	57	n.a.	n.a.	n.a.	n.a.	n.a.	n.a.	n.a.	n.a.	n.a.	n.a.	n.a.	n.a.	46	n.a.
Ce	n.a.	n.a.	32	47	69	136	95	n.a.	n.a.	n.a.	n.a.	n.a.	n.a.	n.a.	n.a.	n.a.	n.a.	n.a.	n.a.	76	n.a.
Ni	174	124	74	83	94	4	145	n.a.	n.a.	n.a.	n.a.	n.a.	112	86	n.a.	n.a.	n.a.	n.a.	n.a.	n.a.	n.a.
Cr	305	252	211	146	160	21	148	n.a.	n.a.	n.a.	n.a.	n.a.	150	76	n.a.	n.a.	n.a.	n.a.	n.a.	120	n.a.
Refer.	\8	\8	\9	\9	\9	\9	\9	\10	\11	\12	\11	\11	\13	\13	\14	\14	\14	\14	\15	\15	\15

Refrences: —**1**= Barberi et al., 1978; Dietrich et al., 1978 (samples DSDP 373 averages of low-Ti, and high Ti lavas) —**2**= Bertrand et al., 1990 (samples ODP 655–1–4, 655–4–1, 655–12–1, 651–44–2, 651–49–1, 651–53–2) —**3**= Selli et al., 1977 (samples: Magnaghi smt. T73–34; Vavilov smt. T72–35–1C; Marsili smt. CT69–27–2A) —**4**= Robin et al., 1987, (average of 3 volatile-free samples, Vavilov smt.) **5**= Beccaluva et al., 1990 (samples ODP 650–67–2, 650–67–2b, 650–69–cc; ODP 654–9–04, 654–9–19) **6**= Savelli and Gasparotto, 1994 (samples M1–3, Vi 1657) —**7**= Keller, 1981 (sample RC–9–2) —**8**= Macciotta et al., 1978 (average of 68 alkaline basalts, and average of 18 subalkaline rocks) —**9**= Cioni et al., 1982 (samples 130, 168, 179, 158, 77 from Monte Arci volcanic complex) —**10**= Deriu et al., 1973 (sample V28A from Monte Ferru volcanic complex) —**11**= Deriu et al., 1974 (samples 423, 239DB, 412 from Monte Ferru volcanic complex) —**12**= Beccaluva et al., 1978 (sample 42 from Monte Ferru) —**13**= Macciotta and Savelli, 1984 (samples LL85, A404 from NW Sardinia) —**14**= Beccaluva et al., 1986 (samples Ha3, Mu4, Tr2, Rh from Aceste smt.) —**15**= Cinque et al., 1988 (samples SH1, 108, 167 from Ustica island).OF=ocean floor; CA= orogenic; IP= intra-plate; ak.b.= alkaline basalt; s.b.= subalkaline basalt; an= andesite; da= dacite; ha= hawaiite; mu.= mugearite; ph= phonolite; rh= rhyolite; te= tephrite; tr= trachyte.

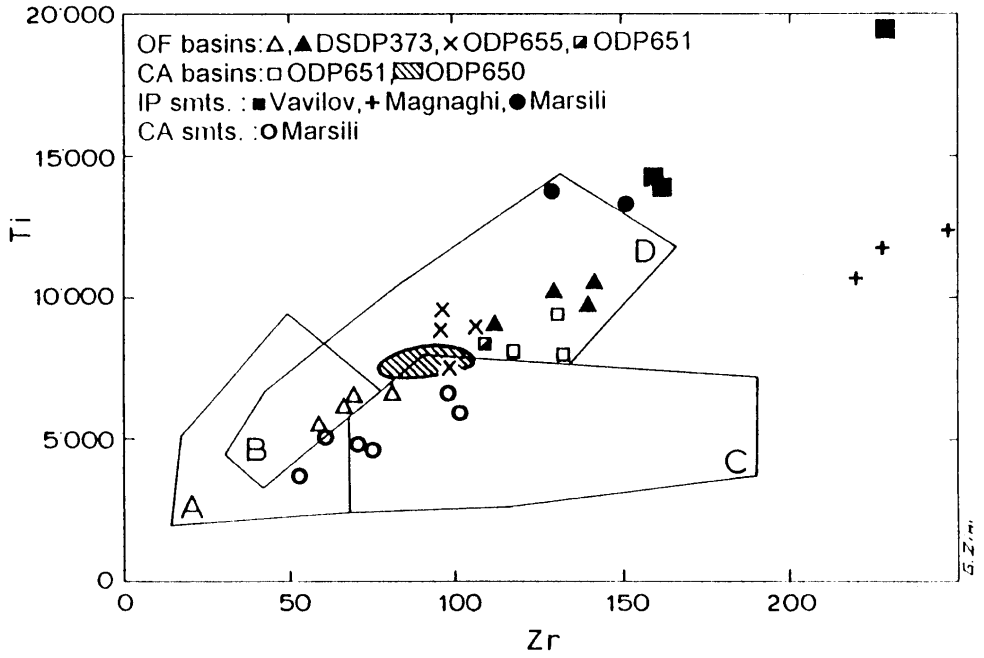

Fig. 5. Ti vs Zr discriminating plot of basalts from the igneous crust of the Vavilov and Marsili basins. Fields (Pearce and Cann, 1973): A = island arc tholeiites, C = calcalkaline basalts, D = ocean floor basalts, B = all three magma types.

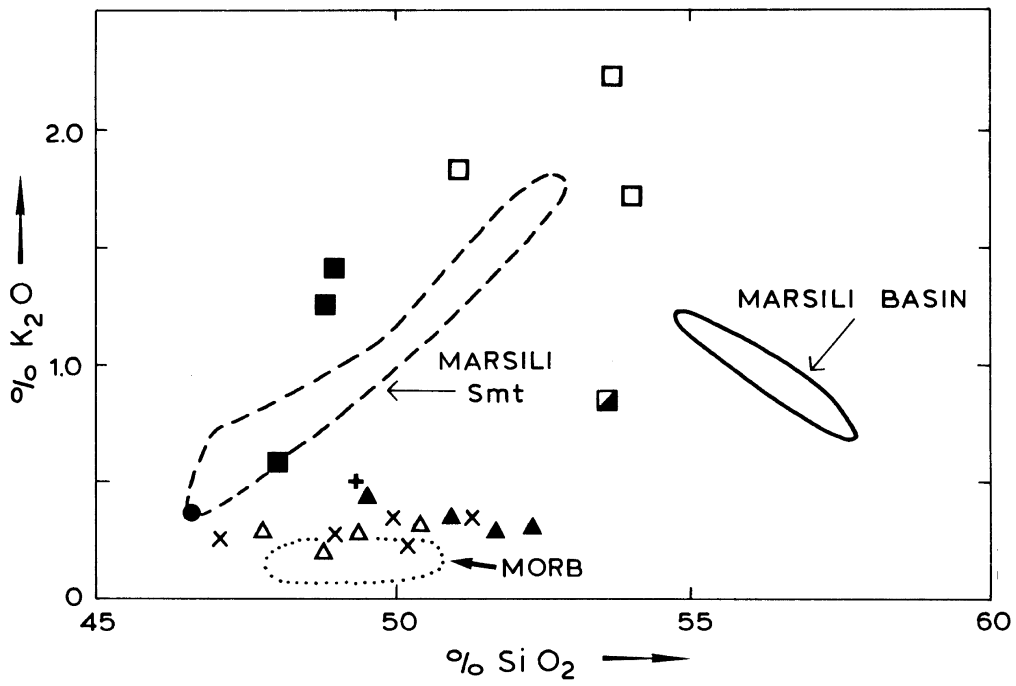

Fig. 6. K_2O–SiO_2 plot of basalts from the igneous crust of the Vavilov and Marsili basins: Symbols as in Fig. 5.

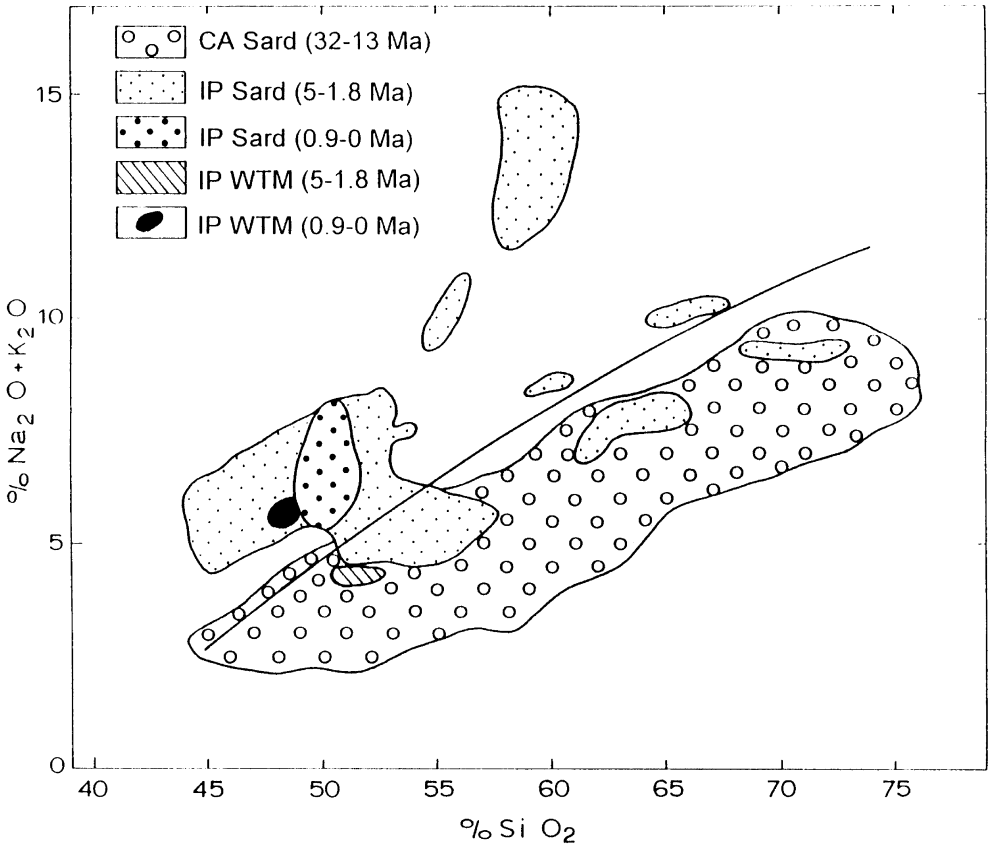

Fig. 7. Alkalies vs SiO_2 discrimination plot of the volcanites from Sardinia and the west Tyrrhenian margin (WTM). Boundary line after Irvine and Baragar (1971).

1988; Savelli, 1988; Bousquet and Lanzafame, 1995). This volcanic island is located between the seamount volcanoes of Anchise to the west and of Sisifo and Enarete to the east. The former forms the southern portion of the supposed intermediate arc of Pliocene age, whereas the latter belongs to the western submerged sector of the Aeolian volcanic arc of the Quaternary episode. The basalt and trachyte lavas and pyroclastites of Ustica have IP, Na-alkalic affinity with an arc signature due to their moderate Ti and Hf contents (Cinque et al., 1988). The Ti–Zr plot (Fig. 9) discriminating between IP and arc lavas (Pearce, 1982) shows that the Ustica volcanites fall outside the field of the subduction-related rocks, differing from the rocks of the adjoining Aeolian and remnant arcs. The different chemistry of the Ustica products is not problematic if one considers an inter-arc emplacement, outside the present subduction zone, and their age which is younger compared to that of the Pliocene remnant arc.

The Aceste seamount, located in the Tyrrhenian southern margin (Fig. 1) yielded lavas of hawaiitic, mugearitic and alkali trachytic compositions and, in addition, rhyolite pyroclastites (Beccaluva et al., 1984). Its age is not younger than the Early Pliocene by biostratigraphic dating of Fe rich clays (Beccaluva et al., 1984). The transitional to weakly alkaline basic lavas of the

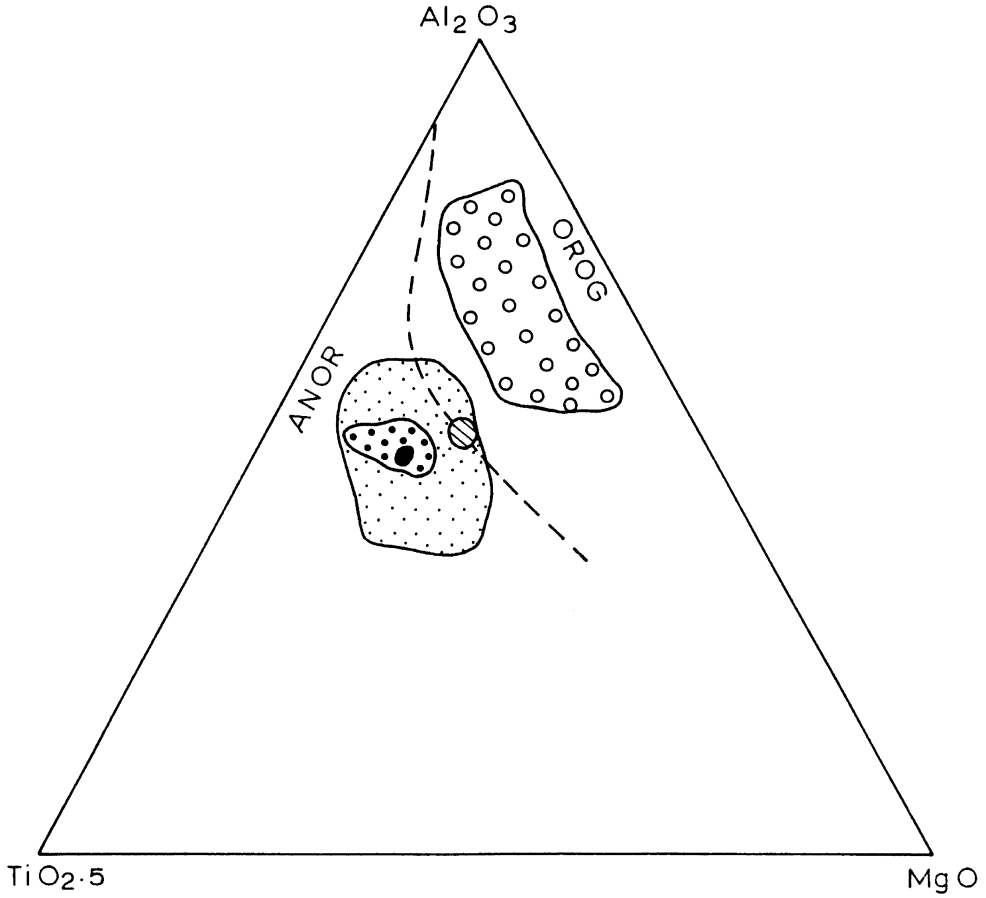

Fig. 8. $TiO_2 \times 5$–Al_2O_3–MgO triangular plot (Cabanis et al., 1990) of the basic and intermediate volcanites from Sardinia and the west Tyrrhenian margin (WTM). OROG = calcalkaline volcanites, ANOR = anorogenic (intra-plate) volcanites. Symbols as in Fig. 7.

seamount are of IP affinity, but also have the subduction-related, geochemical signature of low Nb/Y (<0.8) and Ti/Y (<300) ratios which contrasts with the high Zr values (195 ppm).

The geochemical signatures of both the Aceste and Ustica volcanites may be interpreted in terms of the co-existence of both the island arc and the IP (Na-alkaline) imprintings within the same mantle source. In fact, they have HFSE contents which are only slightly higher than those of the island-arc series, on one side, and, on the other, they show relative depletion of K and Rb, and Na-enrichment. These signatures reflect magma generation from a mantle which has not been strongly modified by the uptake of slab-derived elements like the K and Rb. The displacement of the front of lithosphere convergence and the spaced slab retreat may be responsible for the IP nature of the Aceste and Ustica volcanoes. In fact, their respective sources were located in a distal position relative to the mantle wedges feeding the corresponding volcanic arcs of Pliocene and Quaternary age. Generally, the hybrid volcanism is located in intermediate areas between the western (relict) and the eastern (active) arcs. Slab migration may be invoked to explain the

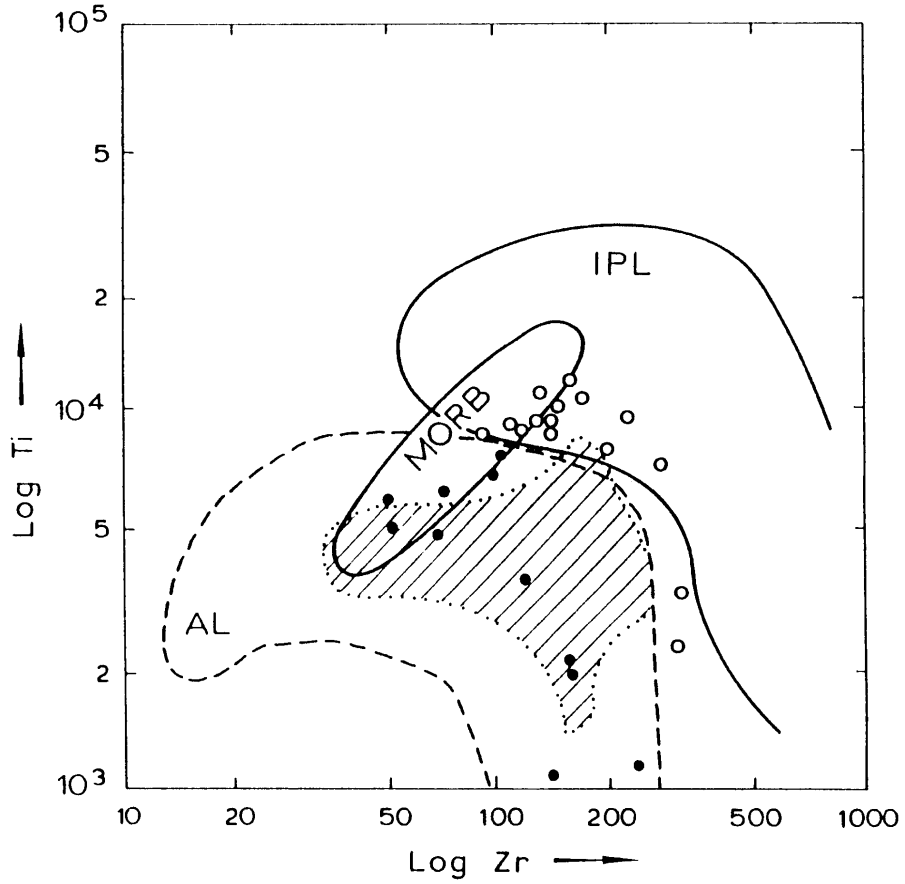

Fig. 9. Log Ti-log Zr binary discrimination diagram (Pearce, 1982) of the volcanites from the 5–1.8 Ma volcanic episode (Pliocene) of the supposed central Tyrrhenian arc(filled circles) and from 1.2–0 Ma volcanic episode (Pleistocene) of the island of Ustica (empty circles). Stripes = representative volcanism of the Aeolian arc. AL = arc volcanites; IPL = post-subduction, IP (alkaline) volcanites.

petrochemical differences existing between the Anchise (orogenic) and the Aceste (anorogenic to transitional) volcanic products during the Pliocene episode, and between the Aeolian (orogenic) and the Ustica (anorogenic to transitional) volcanic products during the Quaternary episode.

The IP volcanism of the STR has a large areal distribution, however its inception is not older than 5 Ma. Typically, anorogenic manifestations are widespread during the post-collision tectonic rejuvenation of the backarc opening (Tarney et al., 1982; Szabo et al., 1992; Pouclet et al., 1995). The post-subduction volcanism of the island of Sardinia, the west Tyrrhenian margin and the ridges of volcanic seamounts, in the Vavilov and Marsili basins, was generated in mantle sources which became slab distant because of the retreat of the convergent boundary.

3.4. Tectonics of the western Tyrrhenian margin

The results obtained by ODP leg 107 have contributed greatly to the unravelling of the tectonic evolution of the Tyrrhenian BAB (Kastens et al., 1988). Stratigraphic data indicate that rifting in

the Tyrrheanian basin propagated from the western margin (Sardinia) to the southeast (Marsili sub-basin). The first documented episode of rifting occurred from late Tortonian to early Messinian on the upper Sardinia slope, followed by a second episode (late Messinian–early Piocene) affecting the lower Sardinia slope. Particular emphasis has been put on this migration of rifting (Kastens and Mascle, 1990; Sartori, 1990; Spadini et al., 1995) although the overall crustal geometry of the western Tyrrhenian margin closely resembles that of a typical passive margin (Malinverno, 1981). In this paper, the lithospheric stretching of the western Tyhhenian margin is considered as a continuous process that lasted from late Tortonian to early Pliocene with the stratigraphy on the Sardinia slope that records the progressive eastwards migration of extension (Kastens et al., 1988). Seismic profiles across the Sardinia margin show that extension was accomplished by block faulting with formation of half grabens (Curzi et al., 1980) and accompanied locally by magmatic effusions (Fabretti et al., 1997).

The stratigraphy of ODP wells 654, 652 and 650 drilled in the Tyrrhenian basin and on its western margin has been backstripped to derive tectonic subsidence curves (Argnani, 1997). The rift related subsidence on the margin (upper Miocene–mid–lower Pliocene) can be seen on the curves obtained from ODP wells 654 and 652, but also a recent episode of subsidence has been documented at about 2 Ma (Fig. 10). This episode of subsidence appears to be basinwide as it can be observed also in the Marsili sub-basin (ODP 650) and occurred well after the end of block faulting on the margin.

4. Discussion

The western Tyrrhenian margin, with its tilted fault blocks and its thinned crust, resembles a typical stretched passive margin. ODP stratigraphy and stratal relationships within half grabens suggest that stretching occurred from late Tortonian to early Pliocene. Datings of basalts recovered in the Vavilov sub-basin fall within the same time interval (8 to 4 Ma), indicating that emplacement of MOR-type basalts occurred during the extension of the western Sardinia margin. This extensional tectonics was followed by some CA activity in the central Tyrrhenian arc and, mainly, by IP volcanism in Sardinia and in the Magnaghi seamount. The second extensional episode, that brought about the opening of the Marsili sub-basin, is not recorded on the western Tyrrhenian margin. Although the structural elements of this last episode of extension are likely to be found on the margins boarding the Marsili sub-basin on the south and east, there is a lack of studies focussing on this aspect, mainly because the large volcanic outpour in this area tends to conceal the structures. However, sediments from well ODP 650 and seismic profiles within the Marsili sub-basin allow us to infer a late Pliocene age for the stretching episode. The basalts emplaced on the basin floor during this extension, sampled only in well ODP 650, have CA affinity, and probably reflect the close proximity to the subducted slab. As in the case of the Vavilov sub-basin, the stretching in the Marsili sub-basin was followed by major CA volcanism in the Aeolian arc and by IP activity in Sardinia, in the Vavilov seamount, in the relict central Tyrrhenian arc and in the upper part of the Marsili seamount.

Taking all the episodes that can be recognised during the evolution of the Tyrhenian basin, two major cycles can be identified, each one composed of two episodes, the first dominated by extension and the second characterised by CA and IP volcanism. The first cycle occurred from 8.5 to 2.5 Ma

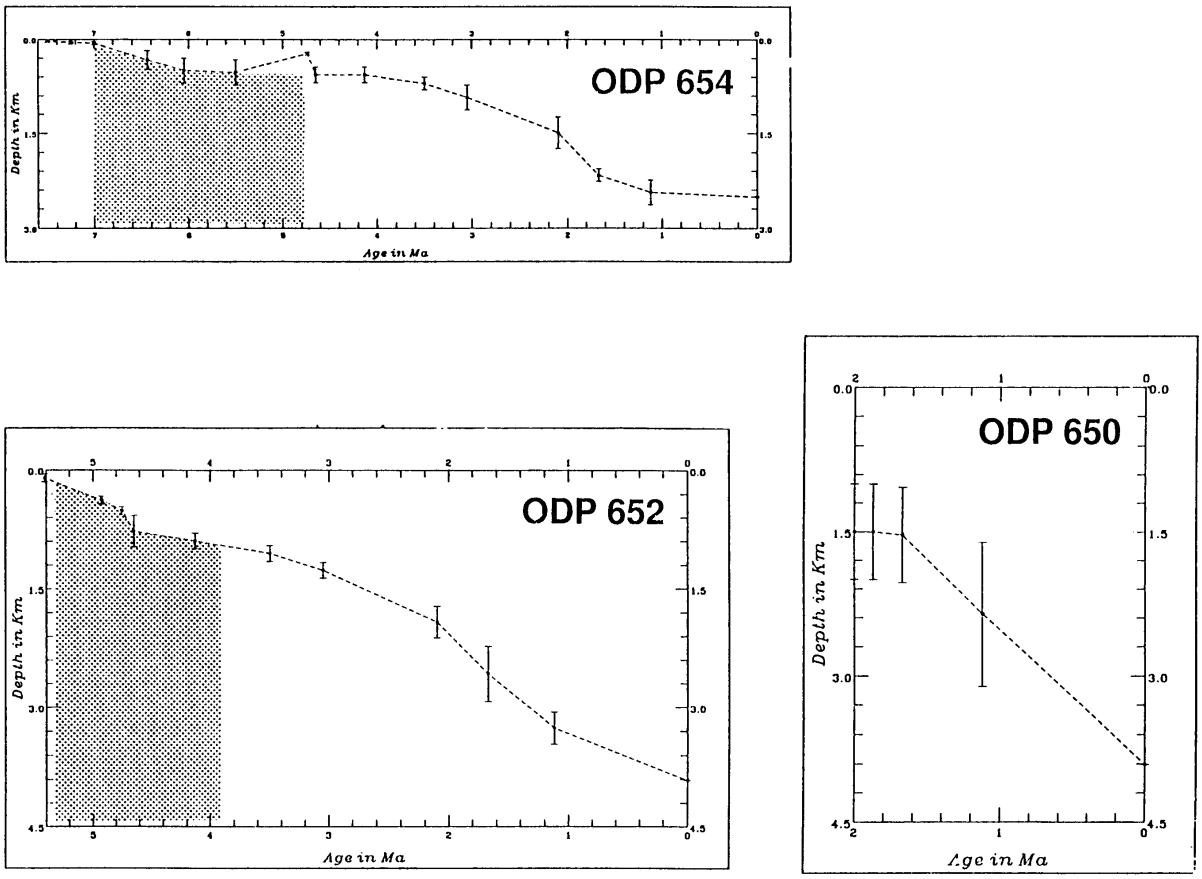

Fig. 10. Subsidence curves for the Tyrrhenian basin and margins. Data from ODP leg 107 wells. The curves represent the tectonic subsidence (total subsidence minus sedimentary load) and the vertical bars the range of paleobathymetric estimates. Gray pattern indicates the duration of syn-rift derived from seismic reflection geometries (After Argnani, 1997).

(late Tortonian to mid Pliocene), and the second, shorter, lasted from 2.0 Ma (late Pliocene) to the Present.

It is considered that this kind of cyclicity could reflect some fundamental geodynamic processes. Times of major trench retreat can give rise to the extensional dominated episodes causing basalts emplacement into the stretched and thinned crust. The nature of the crust of the Vavilov and Marsili sub-basins represents an intriguing problem that, so far, geophysical and petrological data have failed to solve.

The crust that underlies the Vavilov and Marsili sub-basins is quite thin (less than 8 km) but crust of similar thickness has been reported also from highly extended continental basins (Tate et al., 1993), and although E-MORB basalts have been drilled in the Vavilov sub-basin the actual mode of emplacement may be quite different from that operating at mid-ocean ridges. In fact, in the southern Tyrrhenian basin there is no such a feature as a spreading ridge and the irregular magnetic pattern bears little evidence of spreading.

Considering that extensional faulting was active on the western Tyrrhenian margin while the Vavilov sub-basin opened, the emplacement of basalts probably occurred as a dense network of dykes and sills (diffuse spreading; Cochran, 1981) rather than from an eruptive ridge. During these episodes very little volcanism occurs outside the basin.

The slab subducted underneath the Tyrrhenian sea dips very steeply (Selvaggi and Chiarabba, 1995) and is one of the steepest subduction zones known (Isacks and Barazangi, 1977). It is here assumed that the slope of the subducted slab was progressively increasing through time and that this process of slab sinking into the asthenosphere was dominating the episodes were CA and IP volcanism occurred. Slab sinking stirs the mantle (see for instance displacement patterns in Giunchi et al., 1996, Figs 11 and 13) and promotes instability that can interrupt the separation of the convective systems of the lower and upper mantle, favouring the rise of lower mantle melts fertilised by megaliths (Ringwood and Irifune, 1988). The geochemical characters of the IP volcanics seem to be the result of magma generation from a mantle whose composition was not modified by uptake of slab-derived elements. The deep magmatic source is, in fact, in a distal position relative to the mantle wedge overlying the present subduction front. We hypothesize that an upwelling of the lower mantle, induced by, and following, the slab roll-back, can generate the IP imprinting, namely, the elevated HFSE contents and the Na-alkalinity, whereas the overlying mantle (the relict mantle wedge) because of its distal position from the active subduction, does not receive significant geochemical inputs from subduction-derived fluids.

As stretching did not occur or was limited during IP volcanism, basalt emplacement was not diffused into a swarm of fissures. The construction of the major volcanic seamounts, that occured during these episodes, may be due to the fact that basalts erupted from the few major fractures, favouring the build-up of large edifices. Moreover, the along-length linear propagation of the axes of the seamounts might have been impeded by the occurrence of thicker crust on the adjacent basin margins, as it seems to be the case for the Marsili seamount (Faggioni et al., 1995).

The evolution envisaged for the Tyrrhenian backarc basin on the ground of tectonics and magmatic evidence is presented in Fig. 11 and shows alternating episodes of trench retreat and trench stability within the general slab steepening trend. The causes for the change from trench retreat to trench stability are difficult to asses. Certainly, a locking of the subduction margin can stop the trench retreat (Giunchi et al., 1996), but also, considering the overall geometry of the basin, the presence of temporary obstacles along the subduction zone (e.g. impingement of buoyant objects like thick carbonate platforms) could produce the same effect.

The recent (2 Ma) subsidence episode that has been recorded all over the Tyrrhenian basin does not fit easily into subsidence models applied to 'classic' passive margins. This late subsidence is often not considered (e.g. Spadini et al., 1995) although it seems well constrained by paleobathymethic indicators (Hasegawa et al., 1990). Given the backarc setting of the Tyrrhenian basin, it is likely that processes related to subduction contribute to shape the observed tectonic subsidence as cold and dense subducted material is present at depth (Anderson, 1989). The subduction dynamics can also account for the deeper basement observed in backarc basins on a global scale when compared to ocean floors of similar age (Kobayashi, 1984); this observation holds also in the Tyrrhenian basin(Fig. 12). Recent dynamic models of subduction in the Tyrrhenian region seem to support this view that subsidence in a backarc basin is strongly influenced by subduction processes (Giunchi et al., 1996). However, subduction processes should more or less immediately affect the subsidence while the large subsidence observed in the Tyrrhenian basin occurred only in the last 2 Ma and,

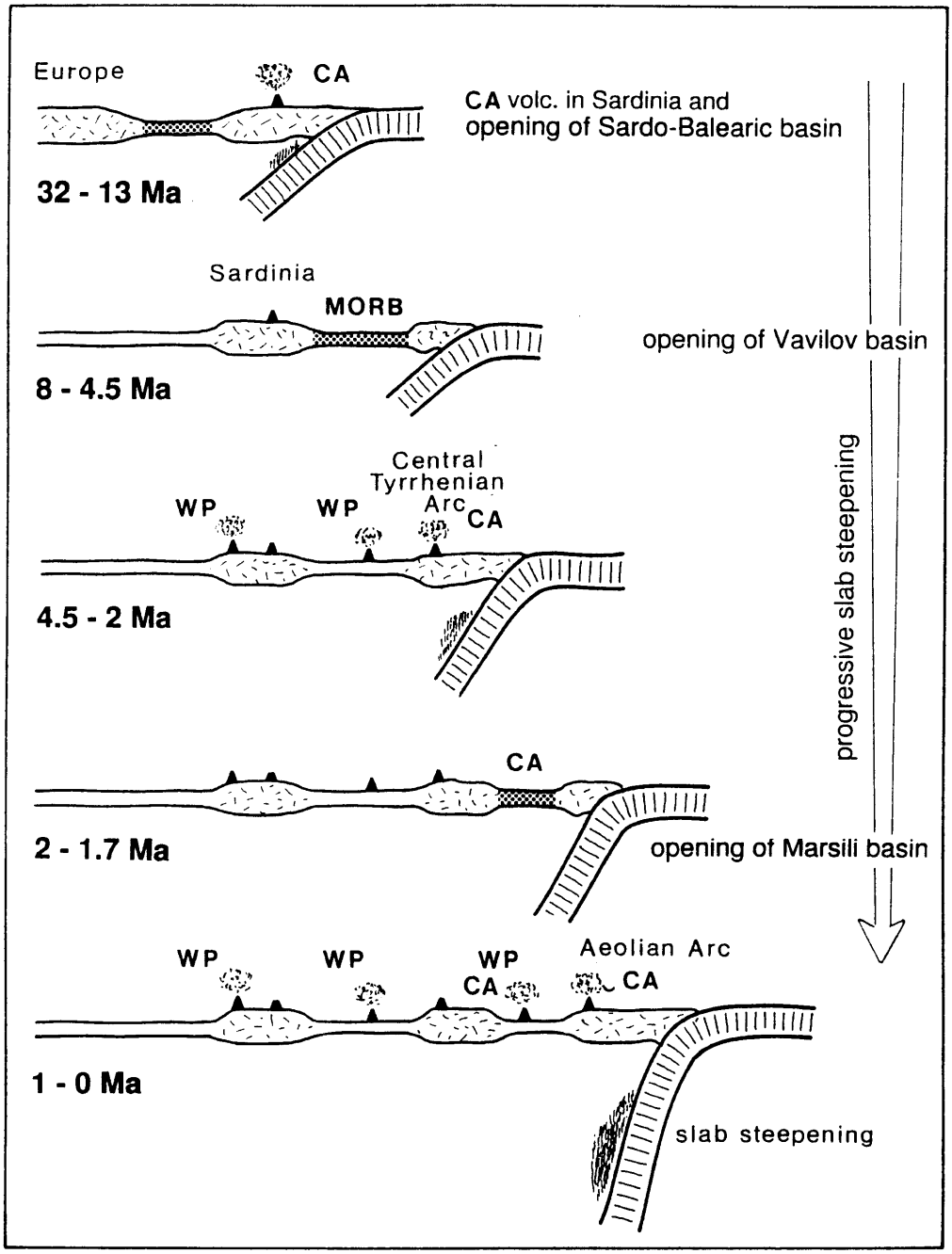

Fig. 11. Proposed geodynamic interpretation of the southern Tyrrhenian basin evolution and space-time distribution of the volcanic episodes in the Sardo–Tyrrhenian region. Sardinia detaches from Europe following the opening of the Sardo–Balearic basin. Slab roll-back and progressive steepening of the subducted lithosphere control the opening of the basinal domains and the nature of magmatic products. Episodes of trench retreat, during which the Vavilov and Marsili sub-basins opened, alternate with episodes of trench stability, during which WP and CA volcanism occur. Also depicted is the general slab steepening trend from the initial shallow subduction (32–13 Ma) to the present steep subduction. CA = Calcalkaline volcanics; MORB = Mid Ocean Ridge Basalts; WP = Within Plate volcanics.

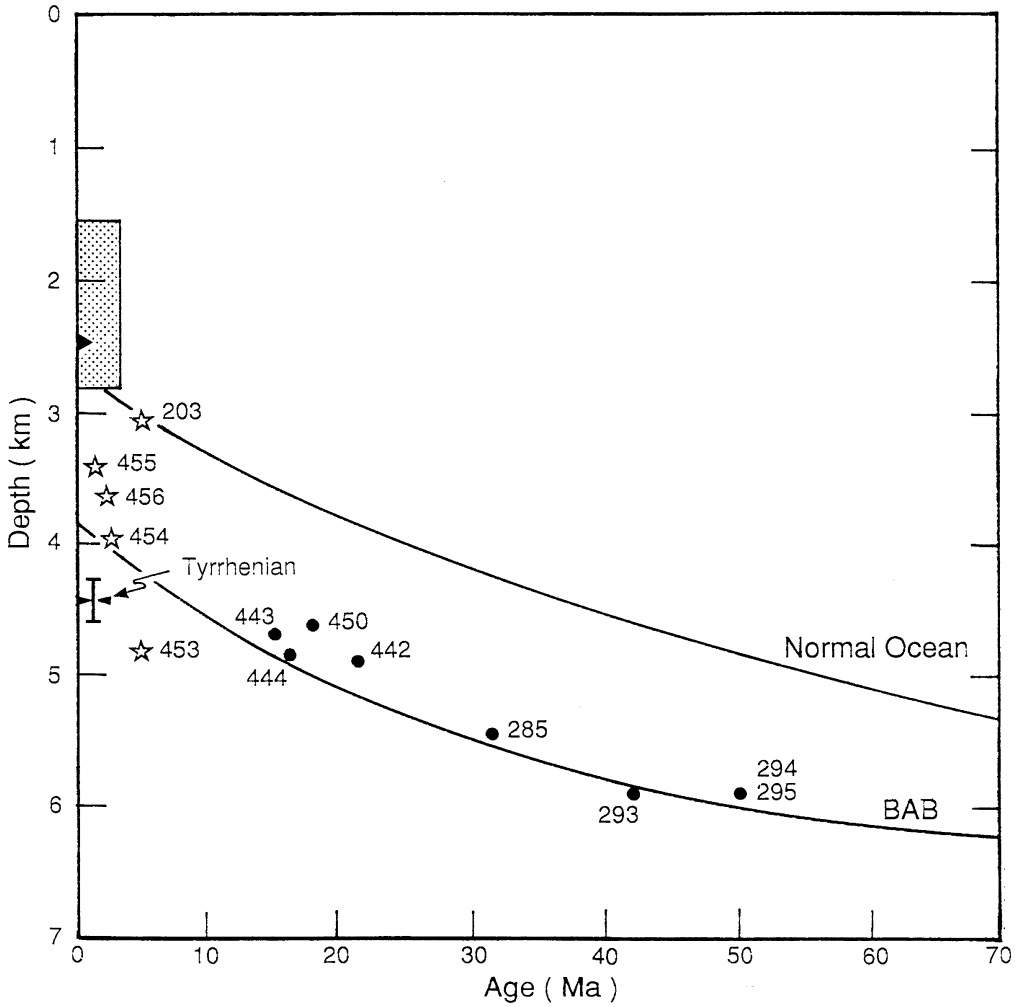

Fig. 12. Comparison between subsidence curves as a function of age for normal oceans and backarc basin (BAB). Numbers refer to DSDP sites. The field of the deep sea floor areas of the Tyrrhenian basin is indicated. Stars and filled dots indicate active and inactive backarc basins, respectively. The gray area represents the depth ranges in Lau basin and Okinawa trough (After Argnani, 1997).

furthermore, it is contemporaneous with the occurrence of large uplift in Calabria (Ghisetti, 1981) and, to a lesser extent, in Sardinia. The Pleistocene uplift of Sardinia is suggested, in the north-western part of the island, by the higher elevation of Pliocene basaltic plateau with respect to the late Pleistocene lava flows that occur within the adjacent valleys (Beccaluva et al., 1981). So far, the relationships between these observables and the geodynamic causes is still far from clear.

5. Conclusions

The nature and timing of tectonic and magmatic events that can be recognised in the Tyrrhenian basin have been reviewed in order to derive a geodynamic model for the evolution of the basin.

The volcanism of the STR may be divided into five episodes whose magmatic products are clearly distinguished based on their magmatic and geodynamic significance, geographic distribution and age (Figs 2 and 3).

Their timings are as follows: **i**) 32–13 Ma (Oligo–Miocene): CA, subduction related volcanism in western Sardinia. **ii**) 8.5–4.5 Ma (Late Miocene–Early Pliocene): sediment covered, ocean floor (OF) basalts of the DSDP Site 373 and ODP Site 655 related to the back-arc opening of the Vavilov basin; sediment covered igneous bodies of the Cornaglia Terrace (not younger than Late Tortonian–Messinian; Fabretti et al., 1997). **iii**) 5–2 Ma (Pliocene): CA volcanism of the intermediate Tyrrhenian arc; IP volcanism in Sardinia, in the passive western Tyrrhenian margin (Site 654, Quirra volcanic seamount), on Aceste seamount and on Magnaghi seamount (Vavilov basin); sediment covered OF (Sites 655 and 651) and CA volcanism (Site 651) in the Vavilov basin. **iv**) 2–1.2 Ma (Latest Pliocene to Early Pleistocene): sediment-covered, CA to OF volcanism (Site 650) related to the opening of the Marsili back-arc basin. **v**) 1–0 Ma (Middle Pleistocene to Holocene): CA volcanism of the Aeolian arc and of the Marsili seamount; IP volcanism in northwestern Sardinia and the passive margin of western Tyrrhenian Sea, on the crest of Marsili seamount, on the crest of Vavilov seamount, and in the island of Ustica, to the east of the remnant intermediate arc.

The five episodes can be grouped into two cycles, each composed of a stretching dominated phase, with magmatism concentrated mainly in the newly created basin floor, followed by calcalkaline volcanism in the arc and intra-plate volcanism oll over the basin. These cycles reflect the geodynamic evolution of the Southern Tyrrhenian backarc basin which appears to be controlled by a back rolling subducted slab that becomes progressively steeper in time Fig. 11. The process of roll back appears to be discontinuous in time with episodes of fast trench retreat, and associated backarc basin stretching, alternating with episodes of steady trench position, and perhaps slab sinking, with associated CA and IP volcanic activity.

Acknowledgements

Jeremy Preston is thanked for his constructive review of the manuscript. Wolfgang Jacoby and two anonymous reviewers greatly contributed to improve the clarity of the paper. L. Casoni and G. Zini carefully looked after the drafting. IGM contribution n. 1130.

References

Anderson D.L., 1989. Theory of the Earth. Blackwell Sci. Publ., Oxford, 366 pp.

Anderson, H., Jackson, J., 1987. The deep seismicity of the Tyrrhenian Sea. Geophysical Journal Royal Astronomical Society 91, 613–637.

Argnani, A., 1990. Modelli sperimentali di tettonica distensiva: implicazioni ed applicazioni. Atti IX Convegno GNGTS, 3–14.

Argnani, A., 1997. Subsidenza tettonica sul margine tirrenico occidentale. Studi Geoloici Camerti 1995/2, 31–39.

Argnani, A., Marani, M., Savelli, C., Galassi, B., 1995. Migrazione del vulcanismo di arco cenozoico ed apertura di piccoli bacini oceanici nel contesto geodinamico intraorogenico del Mar Tirreno meridionale: un riesame. Scritti e Documenti Accademia Nazionale delle Scienze 14, 377–396.

Barberi, F., Innocenti, F., Ferrara, G., Keller, J., Villari, L., 1974. Evolution of Eolian arc volcanism (Southern Tyrrhenian Sea). Earth Planetary Science Letters 21, 269–276.

Barberi, F., Bizouard, H., Capaldi, G., Ferrara, G., Gasparini, P., Innocenti, F., Joron, J.L., Lambert, B., Treuil, M., Allegre, C., 1978. Age and nature of basalts from the Tyrrhenian abyssal plain. Initial Reports DSDP 42I, 509–514.

Beccaluva, L., Deriu, M., Macciotta, G., Savelli, C., Cantoni, M., 1981. Geopetrographic map of the Pliocene–Pleistocene volcanism of NW Sardinia, 1:50,000. Litografia Artistica Cartografica, Firenze.

Beccaluva, L., Morlotti, E., Torelli, L., 1984. Notes on the geology of the Elimi chain area (southwestern margin of the Tyrrhenian Sea). Memorie Societa' Geologica Italiana 27, 213–232.

Beccaluva, L., Bonatti, E., Dupuy, C., Ferrara, G., Innocenti, F., Lucchini, F., Macera, P., Petrini, R., Rossi, P. L., Serri, G., Seyler, M., Siena, F., 1990. Geochemistry and Mineralogy of volcanic rocks from ODP Sites 650, 651, 655 and 654 in the Tyrrhenian Sea. In: Kastens, K.A., Mascle, J., et al. (Eds.), Proceedings of the Ocean Drilling Program. Scientific Results 107, pp. 49–74.

Bertrand, H., Boivin, P., Robin, C., 1990. Petrology and Geochemistry of basalts from the Vavilov Basin(Tyrrhenian Sea), Ocean Drilling Program Leg 107, Holes 651A and 655B. In: Kastens, K.A., Mascle, J., et al. (Eds.), Proceedings of the Ocean Drilling Program. Scientific Results 107, pp. 75–92.

Boccaletti, M., Manetti, P., 1978. The Tyrrhenian sea and adjoining regions. In: Nairn, A.E.M., et al. (Eds.), The Ocean Basins and Margins. Plenum Publ. Corp., New York, vol. 4B, pp. 149–200.

Bousquet, J.C., Lanzafame, G., 1995. Transition from Tyrrhenian basin extension to collisional tectonics: evidence of N–S compression during the recent Quaternary at Ustica. C.R. Acad. Scie. Paris 321IIa, 781–787.

Cabanis, B., Cochemé, J.J., Vellutini, P.J., Joron, J.L., Treuil, M., 1990. Post-collisional Permian volcanism in NW Corsica: an assessment based on mineralogy and trace-element geochemistry. Journal Volcanology Geothermal Research 44, 51–67.

Calanchi, N., Colantoni, P., Gabbianelli, G., Rossi, P.L., Serri, G., 1984. Physiography of Anchise seamount and of the submarine part of Ustica island (South Tyrrhenian): petrochemistry of dredged volcanic rocks and geochemical characteristics of their mantle sources. Mineralogica Petrographica Acta 28, 215–241.

Channell, J.E.T., Mareschal, J.C., 1988. Delamination and asymmetric lithospheric thinning in the development of the Tyrrhenian rift. In: Coward, M.P., Dietrich, D., Park, R.K. (Eds), Alpine Tectonics. Geological Society London, Special Publication 45, pp. 285–382.

Cinque, A., Civetta, L., Orsi, G., Peccerillo, A., 1988. Geology and geochemistry of the island of Ustica. Rendiconti Societa' Italiana Mineralogia Petrologia 43, 987–1002.

Cioni, R., Clocchiatti, R., Di Paola, G., Santacroce, R., Tonarini, S., 1982. Miocene calc-alkaline heritage in the Pliocene post-collisional volcanism of Monte Arci (Sardinia, Italy). Journal Volcanology Geothermal Research 14, 133–167.

Civetta, L., Orsi, G., Scandone, P., Pece, R., 1978. Eastward migration of the Tuscan anatectic magmatism due to anticlockwise rotation of the Apennines. Nature 276, 604–606.

Clift, P.D., ODP Leg 135 Scientific Party, 1995. Volcanism and sedimentation in a rifting island-arc terrain: an example from Tonga, SW Pacific. In: Smellie, J.L. (Ed.), Volcanism Associated with Extension at Consuming Plate Margins. Geological Society Special Publication 81, pp. 29–51.

Cochran, J., 1981. The gulf of Aden: structure and evolution of a young ocean basin and continental margin. Journal Geophysical Research 86 (B1), 263–287.

Crisci, G.M., De Rosa, R., Esperanza, S., Mazzuoli, R., Sonnino, M., 1991. Temporal evolution of a three component system: the island of Lipari (Eolian Arc, southern Italy). Bulletin Volcanology 53, 207–221.

Curzi, P., Fabbri, A., Nanni, T., 1980. The Messinian evaporitic event in the Sardinia basin area (Tyrrhenian Sea). Marine Geology 34, 157–170.

Della Vedova, B., Pellis, G., Foucher, J.P., Rehault, J.P., 1984. Geothermal structure of the Tyrrhenian Sea. Marine Geology 55, 271–289.

Deriu, M., Di Battistini, G., Macciotta, G., Venturelli, G., 1973. Manifestazioni vulcaniche periferiche nel Moniferro sud-occidentale. Bollettino Societa' Geologica Italiana 92, 713–759.

Deriu, M., Di Battistini, G., Gallo, F., Giammetti, F., Vernia, L., Zerbi, M., 1974. Caratteri geopetrografici del Montiferro centrale (Sardegna). Memorie Societa' Geologica Italiana 13/2, 415–439.

Dickinson, W.R., 1975. Potash-depth (K-h) relations in continental margins and intra-oceanic magmatic arcs. Geology 3, 53–56.

Dietrich, V., Emmermann, H., Puchelt, H., Keller, J., 1978. Oceanic basalts from the Tyrrhenian basin, DSDP Leg 42A, Hole 373A. Initial Reports DSDP 42/I, 515–530.

Doglioni, C., 1991. A proposal of kinematic modeling for W-dipping subductions—Possible applications to the Tyrrhenian–Apennines system. Terra Nova 3, 423–434.
Fabretti, P., Sartori, R., Torelli, L., Zitellini, N., Brancolini, G., 1997. La struttura profonda del margine orientale della Sardegna. Studi Geologici Camerti 1995/2, 239–246.
Faggioni, O., Pinna, E., Savelli, C., Schreider, A.A., 1995. Geomagnetism and age study of Tyrrhenian seamounts. Geophysical Journal International 123, 915–930.
Ferrari, L., Manetti, P., 1993. Geodynamic framework of the Tyrrhenian volcanism: a review. Acta Vulcanologica 3, 1–9.
Ghisetti, F., 1981. Upper Pliocene–Pleistocene uplift rates as indicators of neotectonic pattern: an example from southern Calabria (Italy). Zeitung Geomorphologie N. F. (Suppl.-Bd.) 40, 93–118.
Giardini, D., Velona', M., 1991. The deep seismicity of the Tyrrhenian Sea. Terra Nova 3, 57–64.
Giunchi, C., Sabadini, R., Boschi, E., Gasperini, P., 1996. Dynamic models of subduction: geophysical and geological evidence in the Tyrrhenian Sea. Geophysical Journal International 126, 555–578.
Hasegawa, S., Sprovieri, R., Poluzzi, A., 1990. Quantitaive analysis of benthic foraminifera assemblages from Plio–Pleistocene sequences in the Tyrrhenian Sea, ODP Leg 107. In: Kastens, K.A., Mascle, J., et al. (Eds.), Proceedings of the ODP. Scientific Results 107, pp. 461–478.
Hole, M.J., Saunders, A.D., Rogers, G., Sykes, M.A., 1995, The relationship tetween alkaline magmatism, lithospheric extension and slab window formation along continental destructive plate margins. In: Smellie, J.L. (Ed.), Volcanism Associated with Extension at Consuming Plate Margins. Geological Society Special Publication 81, pp. 265–285.
Innocenti, F., Manetti, P., Mazzuoli, R., Villari, L., 1983. Vulcanismo nelle zone di collisione continentale: l'esempio del Mediterraneo orientale. Rendiconti Societa' Italiana Mineralogia Petrologia 38/3, 1027–1041.
Irvine, T.N., Baragar, W.R.A., 1971. A guide to the chemical classification of the common volcanic rocks. Canadian Journal Earth Sciences 8, 523–548.
Isacks, B.L. and Barazangi, M., 1977. Geometry of Benioff zones: lateral segmentation and downwards bending of the subducted lithosphere. In: Talwani, M., Pitman, W.C. (Eds.), Island arcs, Deep-Sea Trenches and Back-Arc Basins. American Geophysical Union, Maurice Ewing Series 1, pp. 99–114.
Jakes, P., White, A.R., 1972. Major and trace element abundances in volcanic rocks of orogenic areas. Geological Society America Bulletin 83, 29–40.
Kastens, K., Mascle, J., et al., 1988. ODP Leg 107 in the Tyrrhenian sea: Insights into passive margin and back-arc basin evolution. Geological Society America Bulletin 100, 1140–1156.
Kastens, K.A., Mascle, J., 1990. The geological evolution of the Tyrrhenian Sea: an introduction to the Scientific results of ODP Leg 107. In: In: Kastens, K.A., Mascle, J. et al. (Eds.), Proceedings of the ODP. Scientific Results 107, pp. 3–26.
Keller, J., 1981. Alkalibasalts from the Tyrrhenian sea basin: magmatic and geodynamic significance. Bulletin Volcanology 44/3, 327–337.
Kobayashi, K., 1984. Subsidence of the Shikoku Back-Arc Basin. Tectonophysics 102, 105–117.
Lavecchia, G., 1988. The Tyrrhenian-Apennines system: strucural setting and seismotectogenesis. Tectonophysics 147, 263–296.
Locardi, E., Nicolich, R., 1992. Geodinamica del Tirreno e dell'Appenino centro-meridionale: la nuoca carta della Moho. Memorie Societa' Geologica Italiana 41, 121–140.
Macciotta, G., Savelli, C., 1984. Petrology and K/Ar ages of Pliocene–Quaternary volcanics from northwestern Sardinia. Grafiche STEP, Parma, Pre-print, 45p.
Malinverno, A., Ryan, W.B.F., 1986. Extension in the Tyrrhenian Sea and shortening in the Apennines as result of arc migration driven by sinking in the lithosphere. Tectonics 5, 227–245.
Mantovani, E., Albarello, D., Babbucci, D., Tamburelli, C., 1992. Recent geodynamic evolution of the central Mediterranean region (Tortonian to Present). Tipografia Senese 00, 88.
Mongelli, F., Cataldi, R., Celati, R., Della Vedova, B., Fanelli, M., Nuti, S., Pellis, G., Squarci, P., Taffi, L., Zito, G., 1992. Geothermal regime in Italy. In: Hurtig, E., Cermak, V., Haenel, R., Zui, V. (Eds.), Geothermal Atlas of Europe. H. Haack Verlagsges Gotha, pp. 54–59.
Nicolich, R. and Dal Piaz, G.V., 1991. Isobate della moho in italia. In: Structural Model of Italy, 1:500.000, Progetto Finalizzato Geodinamica. CNR, Roma.

Patacca, E., Scandone, P., 1989. Post-Tortonian mountain building in the Apennines. The role of passive sinking of a relic lithospheric slab. The lithosphere in Italy, Mid Term Conference, Rome 5–6 May 1987. Atti Convegni Accademia Nazionale dei Lincei, n. 80, pp. 157–176.

Patacca, E., Sartori, R., Scandone, P., 1992. Tyrrhenian basin and Apenninic arcs. Kinematic relations since late Tortonian times. Memorie Societa' Geologica Italiana 45, 425–451.

Pearce, J.A., 1982. Trace element characteristics of lavas from destructive plate boundaries. In: Thorpe, R.S. (Ed.), Andesites. John Wiley and Sons, pp. 525–548.

Pouclet, A., Lee, J.S., Vidal, P., Cousens, B., Bellon, H., 1995. Cretaceous to Cenozoic volcanism in South Korea and in the Sea of Japan: magmatic constraints on the opening of the back-arc basin. In: Smellie, J.L. (Ed.), Volcanism associated with extension at consuming plate margins. Geological Society Special Publication 81, pp. 169–191.

Ringwood, A.E., Irifune, T., 1988. Nature of the 650 km seismic discontinuity: implications for mantle dynamics and differentiation. Nature 331, 131–136.

Robin, C., Colantoni, P., Gennesseaux, M., Rehault, J.P., 1987. Vavilov seamount: a mild alkaline Quaternary volcano in the Tyrrhenian basin. Marine Geology 78, 125–136.

Sartori, R., 1990. The main results of ODP Leg 107 in the Frame of Neogene to recent geology of Perityrrhenian areas. In: Kastens. K.A., Mascle, J., et al. (Eds.), Proceedings of the ODP. Scientific Results 107, pp. 715–730.

Savelli, C., 1984. Evoluzione del vulcanismo cenozoico (da 30 Ma al Presente) nel Mar Tirreno e nelle aree circostanti: ipotesi geocronologica sulle fasi dell'espansione oceanica. Memorie Societa' Geologica Italiana 27, 111–119.

Savelli, C., 1988. Late Oligocene to Recent episodes of magmatism in and around the Tyrrhenian Sea: Implications for the processes of opening in a young inter-arc basin of intra-arc-orogenic (Mediterranean) type. In: Wezel, F.C. (Ed.), The Origin of Arcs. Tectonophysics 146, pp. 163–181.

Savelli, C., Beccaluva, L., Deriu, M., Macciotta, G., Maccioni, L., 1979. K-Ar geochronology and evolution of the Tertiary 'calc-alkalic' volcanism of Sardinia (Italy). Journal Volcanology Geothermal Research 5, 257–269.

Scott, R., Kroenke, L., 1980. Evolution of back-arc spreading and arc volcanism in the Philippine sea: Interpretation of Leg 59 DSDP results. In: Hayes, D.E. (Ed.), The geologic and tectonic evolution of SE Asian seas and islands. American Geophysical Union. Monograph 23, pp. 247–268.

Selli, R., Lucchini, F., Rossi, P.L., Savelli, C., Del Monte, M., 1977. Dati geologici, petrochimici e radiometrici sui vulcani centro tirrenici. Giornale Geologia 42, 221–246.

Selvaggi, G., Chiarabba, C., 1995. Seismicity and P-wave image of the southern Tyrrhenian subduction zone. Geophysical Journal International 121, 818–826.

Serri, G., 1990. Neogene–Quaternary magmatism of the Tyrrhenian Region: characterization of the magma sources and geodynamic implication. Memorie Societa' Geologica Italiana 41, 219–242.

Spadini, G., Cloetingh, S., Bertotti, G., 1995. Thermo-mechanical modeling of the Tyrrhenian Sea: Lithospheric necking and kinematics of rifting. Tectonics 14, 629–644.

Steinmetz, L., Ferrucci, F., Hirn, A., Morelli, C., Nicolich, A., 1983. A 550 km long Moho traverse in the Tyrrhenian Sea from OBS recorded PN waves. Geophysical Research Letters 6, 428–431.

Szabo, C., Harangi, S., Csontos, L., 1992. Review of Neogene and Quaternary volcanism of the Carpathian–Pannonian region. Tectonophysics 208, 243–256.

Tarney, J., Weaver, S.D., Saunders, A.D., Pankhurst, R.J., Barker, P.F., 1982. Volcanic evolution of the N Antarctic peninsula and the Scotia arc. In: Andesites. J Wiley and Sons, pp. 371–400.

Tate, M., White, N., Conroy, J.-J., 1993. Lithospheric Extension and Magmatism in the Porcupine Basin West of Ireland. Journal Geophysical Research 98, 13905–13923.

Uyeda, S., 1982. Subduction zones: an introduction to comparative subductology. Tectonophysics 81, 133–159.

Wang, C.Y., Hwang, W.T., Shi, Y., 1989. Thermal evolution of a Rift basin: the Tyrrhenian Sea. Journal Geophysical Research 94, 3991–4006.

Wezel, F.C., 1985. Structural features and basin tectonics of the Tyrrhenian Sea. In: Stanley, D.J., Wezel F.C. (Eds.), Geological Evolution of the Mediterranean basin. Springer Verlag, pp. 153–194.

Yilmaz, Y., 1990. Comparison of young volcanic associations of western and eastern Anatolia formed under a compressional regime. Journal Volcanology Geothermal Research 44, 69–87.